Research Square

Preprints are preliminary reports that have not undergone peer review.
They should not be considered conclusive, used to inform clinical practice,
or referenced by the media as validated information.

Enhanced Magnetoelectric coupling in Praseodymium doped multiferroïc bismuth ferrites

A. AMOURI

amouri.amira00@gmail.com

University of Gabes

D. Dhruv

Saurashtra University

W. DIMASSI

Laboratory of Nanomaterials and Systems for Renewable Energy of Research and Technology Center of Energy, Borj-Cedria Science and Technology Park, BP 95, Hammam-Lif 2050, Tunisia.

Research Article

Keywords: Multiferroïcs, Ceramics, Bismuth ferrite, Magnetic, Ferroelectric, Magnetoelectric coupling

Posted Date: May 5th, 2026

DOI: https://doi.org/10.21203/rs.3.rs-9331060/v1

License: This work is licensed under a Creative Commons Attribution 4.0 International License.
Read Full License

Additional Declarations: No competing interests reported.

Version of Record: A version of this preprint was published at Journal of Materials Science: Materials in Electronics on August 13th, 2026. See the published version at https://doi.org/10.1007/s10854-026-18235-3.

Enhanced Magnetoelectric coupling in Praseodymium doped multiferroïc bismuth ferrites

A. AMOURI*[1, 2],D. Dhruv[3], W. DIMASSI[1]

[1] Laboratory of Nanomaterials and Systems for Renewable Energy of Research and Technology Center of Energy, Borj-Cedria Science and Technology Park, BP 95, Hammam-Lif 2050, Tunisia.
[2] University of Gabes, Preparatory Institute for Engineering Studies in Gabès IPEIGb, Avenue Omar Ibn El Khattab, Zrig Eddakhlania Gabes 6029, Tunisia.
[3] Department of Physics, Saurashtra University, Rajkot 360005, Gujarat, India.

Corresponding author: E-mail address: amouri.amira00@gmail.com

Abstract

The polycrystalline $Bi_{1-x}Pr_xFeO_3$ ceramic synthesis was obtained through a solid-state reaction under a controlled atmosphere. The X-ray diffraction Rietveld refinement showed a rhombohedral R3c structure for all our ceramics. Room temperature M vs. H and P vs. E hysteresis loops revealed improved magnetic and ferroelectric properties due to Praseodymium substitution. The $Bi_{0.95}Pr_{0,05}FeO_3$ ceramic presents attainable saturated hysteresis loops with a spontaneous polarization (P_s) of 18.05 μC/cm^2. Pr substitution enhances magnetization, reaching the uppermost remnant magnetization (M_r) of 6.73 emu/g for x = 0.025 composition. Moreover, Both T_c and T_N shifted closer to room temperature and approached each other for $Bi_{0.975}Pr_{0,025}FeO_3$ ceramics, indicating enhanced magnetoelectric coupling. At room temperature, the highest value of α_{ME} was obtained for the optimum $Bi_{0.975}Pr_{0,025}FeO_3$ ceramic: before electrical poling, α_{ME} was of 1.526 mVcm^{-1}Oe^{-1}. The interesting features suggest the $Bi_{0.975}Pr_{0,025}FeO_3$ magnetoelectric ceramics as a potent candidate for a wide span of modern applications

Keywords: Multiferroïcs; Ceramics; Bismuth ferrite; Magnetic; Ferroelectric; Magnetoelectric coupling.

I. Introduction

The ferroïc properties combined in the same phase have made multiferroïc materials of growing interest for multiples innovative technological applications **[1-6]**. Notably, simultaneous ferroelectric and magnetic order parameters in the same phase have been proved highly useful for next generation multifunctional devices **[3-5,7-19]**. Beside the unavailability of commercial measurement systems studying the magnetoelectric effect and the non-existence of standard well defined measuring techniques **[7-9]**, interaction failure among ferroïc order parameters resulting on weak magneto-electric coupling for the most multiferroïc **[7-8]** made the study of such coupling interesting. In fact, other methods already used to prove the magnetoelectric properties and the improvement of this coupling pass indirectly through the magnetoelastic properties. Crystal symmetries, coupling constants, and ordered patterns provide numerous opportunities to discover and design materials exhibiting strong magnetoelectric coupling **[10]**. So, by combining piezoresponse force microscopy and magnetic force microscopy, F. Yan et al. **[11]** were able to quantitatively measure magnetoelastic strain-driven responses in thin-film nanocomposites, providing insights into local mapping of magnetoelectric coupling. Also, I. Kallel et al. **[12]** revealed the presence of magnetoelectric coupling via studying the total polarization obtained from Rietveld refined atomic positions: the coupled evolution between the deduced total polarization and the magnetic ordering was mediated by magnetoelastic coupling.

As one of the multiferroïc magnetoelectric materials, $BiFeO_3$ (BFO) has been valued for ferroelectric and magnetic ordering coexistence at room temperature **[14]**. BFO exhibits high phase transition temperatures: ferroelectric Curie temperature T_c ~ 1100 K and G-type antiferromagnetic ordering temperature T_N ~ 643K **[15-18]**. The material crystallizes in a Rhombohedral distorted perovskite structure with an R3c space group: the ferroelectricity is mainly due to displacements of the lone pair $6s^2$ of Bi^{3+} **[16-17]**. The magnetic property is the result of the Fe-O-Fe super-exchange interactions: the G-type antiferromagnetic ordering with a long-range spin cycloid with a period of 62 nm is attributed to the transition metal cation Fe^{3+}. The spiral arrangement of the magnetic moments of Fe^{3+} ions and the canted spins due to Dzyaloshinskii–Moriya (DM) interaction are at the origin of weak ferromagnetic order **[16-17]**. However, the performance of BFO is still limited for multiples applications **[1-5]** due to its high leakage current, low dielectric constant, weak magnetic moments, spiral spin behavior and weak ME coupling **[17, 20-24]**. In fact, even if the dynamic magnetoelectric measurements for the $xBiFeO_3$-$(1 - x)NiFe_2O_4$ nanocomposite has been recorded, T. Ichinose et al. **[13]** observed just a quadratic response of the ferroelectric polarization hysteresis loops

as a function of the magnetic field. To improve BFO parent compound physical properties, previous contributions have suggested alternative strategies **[7-9, 18, 22--39]**. Thus, a way to improve the physical properties and especially having a stronger ME coupling is to have suitable doping with ABO_3 solid solution **[17, 25-28]** and/or substitution with appropriate element(s), essentially, rare-earth (RE) ions **[7-9, 22-24, 29-33]** at the Bi/Fe site(s) of BFO. In this context, we study the effect of Praseodymium (Pr) substitution in $BiFeO_3$ parent compound on ferroelectric, magnetic properties and especially, magnetoelectric coupling. The choice of the Praseodymium (P_r) doping was based on previous research works, reporting the improvement of ferroelectric, magnetic and photovoltaic properties of solid solution based on $BiFeO_3$ as an effect of Pr substitution **[34-39]**. In fact, A. S. Kumar et al. **[30]**, while studding $Bi_{1-x}Pr_xFeO_3$ solid solution, shows the increase of the dielectric constant values and the enhancement of the magnetization values with Pr doping to reach a value of 0.5 emu/g for the optimal composition $Bi_{0.8}Pr_{0.2}FeO_3$ ceramic **[34]**. V. Verma et al. **[38]**, during his study of the same system, synthesized by the sol-gel technique, with $0 \leq x \leq 0.25$ compositions in step of 0,05, show the improvement of both ferromagnetic and ferroelectric properties and indicates a probable correlation between such physical enhancement properties with the structural transformation and grain morphology. In the same context, N. Kumar et al **[46]** studied Pr substituted $Bi_{1-x}Pr_xFeO_3$ ($0 \leq x \leq 0.15$) multiferroïc compounds, highlighted a higher polarization for the Pr substituted system with a growth in the saturation polarization reaching a value of 0.223 $\mu C/cm^2$ under an applied field of 15.311 kV/cm for $Bi_{0.85}Pr_{0.15}FeO_3$ compound **[46]**, while, a near linear field dependence signature of the persisting of the antiferrromagnetic behavior of $BiFeO_3$ parent sample is observed **[46]**. Also, X. Li et al. **[42]** proved the coexistence of magnetism and ferroelectricity at room temperature for Pr and Co co-substituted $BiFeO_3$ nanoparticles. The improvement of both magnetic and ferroelectric properties was linked to structural transition by incorporating Pr in the $BiFeCo_{0,05}O_3$ **[39]**. Despite numerous studies of the effect of Pr in both magnetic and ferroelectric properties of $BiFeO_3$ parent compound **[34-37]**, the magnetoelectric coupling in such system have not been evoked, yet, only through the magnetoelastic properties **[10-12]**. Therefore, in the present report, the polycrystalline $Bi_{1-x}Pr_xFeO_3$ ceramic system with $0 \leq x \leq 0,05$ compositions are synthesized by a solid-state reaction method under a controlled atmosphere and the impact of Praseodymium (P_r) doping on the structural, magnetic, ferroelectric properties and the magnetoelectric coupling of our synthesized ceramics has been investigated. Significant improvement in the magnetoelectric response has been observed with best magnetoelectric coupling for the optimal composition $Bi_{0.975}Pr_{0,025}FeO_3$ (x = 0,025).

II. Experimental details

Polycrystalline ceramic system $Bi_{1-x}Pr_xFeO_3$ with $0 \leq x \leq 0{,}05$ compositions synthesis was performed by the solid-state reaction method under a controlled atmosphere. The stoichiometric amounts of the precursors (99.9% purity) were as follows: Bismuth oxide Bi_2O_3 (Aldrich), Praseodymium oxide Pr_2O_3 (Aldrich) and Iron oxide Fe_2O_3 (Aldrich). Powders were wet milled in an agate jar by agate balls (3 mm diameter) for 12 h at a rotation speed of 600 t/mn. Dried samples were shaped under uniaxial pressing of 20 bar for one minute into pellets of 13 mm in diameter, calcined at 873 K during 12 h under a controlled atmosphere and milled again for 12 h. The powder was subsequently shaped into pellets of 8 mm in diameter by uniaxial pressing of 20 bar for one minute. The products underwent a second heat treatment and were sintered in a furnace heated from 1173 K to 1273 K for 1 h under a controlled atmosphere. The density of the pellets was higher than 98% according to Archimedes method. The purity phases and the structure were identified via X-Ray diffraction (XRD) patterns recorded with a Panalytical X'PERT Pro diffractometer with CuK_α radiation (λ = 1.5406 Å) at room temperature. The data were collected in the angle range of $20° < 2\theta < 90°$ with 10 s counting time for each step of 0.02° step. For X-ray diffraction pattern Rietveld refinement, the Fullprof software **[41]**. The crystal Structures, cell parameters and the interatomic distances and bond angles were determined allowing the establishing of the association between structural distortion and magnetic and ferroelectric properties evolution. Magnetization properties were revealed using a Quantum Design MPMS-XL-7CA SQUID magnetometer. Zero field cooled (ZFC) and field cooled (FC) magnetization curves were obtained at 0,05 T in the temperature range 5-400K. Magnetization curves were recorded at 300 K. The ferroelectric polarization P-E hysteresis loops were quantified in a silicone oil bath equipped with a Sawyer-Tower circuit and a linear variable differential transformer, at room temperature at a frequency of 10 Hz. Room-temperature magnetoelectric ME responses appeared under an applied magnetic field H_{DC} varying in the range from 0.00 Oe to 0.45 Oe with H_{AC} equal to 0.0005 T at 1 kHz.

III. Results and discussions

1. Structural properties

The XRD for $BiFeO_3$ parent compound and $Bi_{1-x}Pr_xFeO_3$ solid solution with x = 0,025 and 0,05 compositions was carried out at room temperature. The choice of low substitution of bismuth by Praseodymium was based in previous research works **[37-38]** to have rhombohedral lattice type for doped samples, keeping that of $BiFeO_3$ parent compound. In fact, the improvement of both magnetic and ferroelectric properties was linked to structural transition due to the incorporation of Pr into $BiFeO_3$ **[37-38]**. So, the idea is to study the effect of Pr substitution into $BiFeO_3$ in magnetoelectric properties and especially it's effect to the order of coupling, while preserving the same rhombohedral lattice structure like $BiFeO_3$ parent compound. As shown in Fig.1, all diffractograms show clearly intense hkl peaks which proves the perfect crystallization and the absence of parasite phase in all samples, except for $BiFeO_3$ ceramics. In fact, for $BiFeO_3$ parent compound, the XRD images displayed low intensity peaks which correspond to the $Bi_{25}FeO_{49}$ and $Bi_2Fe_4O_9$ impurity phases (as shown by asterisks in Fig. 2(a)). The intense peak of the principal phase ratio by that of the impurity was around 0.16 %. In the doped samples, we excluded the growth of such impurity phases. Fig.1 shows the superposition of all diffractograms. The identification of the hkl peaks relied on the database of «X-PertHighScore». As expected, for all our prepared ceramics, the peaks could be indexed based on rhombohedral R3c space group symmetry, accordance with the JCPDS 01-072-2112, like $BiFeO_3$ parent compound. In fact, while keeping hkl peaks corresponding to rhombohedral symmetry, a notable change in the hkl ratio intensity peaks is detected: This behavior illustrates an isostructural distortion as a result of the Praseodymium substitution. In fact, In addition to the shift in 2θ that will be discussed later, Fig.1 illustrate a change in the ratio intensity between the peak (104) in the left and (110) on the right, as the Praseodymium substitution rate increase, and a remarkable broadening, especially for $Bi_{0.95}Pr_{0,05}FeO_3$ (x = 0,05), is noted. In fact, the intensity of the peak (104) reduces and the lined-width of the peak (110) broadened. R. A. M. Gotardo et al. **[16]** reported similar results, while studding $BiFeO_3$-$BaTiO_3$ solid solutions, and attributed this behavior to a distorted perovskite structure with the coexistence of rhombohedral and monoclinic symmetry as the $BaTiO_3$ concentration increased. R. Dahiya et al. **[42]** outline that all the samples crystallized in rhombohedral distorted perovskite structure, while studding the effect of Sr and V doping in $BiFeO_3$ multiferroïc properties: Thus, the monotonous change observed for the diffraction peaks, indicating a gradual isostructural lattice distortion, has been discussed as origination from the effect of the difference in ionic radius and the charge compensation mechanisms. Therefore, in our case, such behavior indicate a progressive isostructural distortion of the unit cell due to the increase of Praseodymium substitution rate: The monotonous lattice distortion while maintaining Rhombohedral structure could be discussed as the effect of the variation of the average radii of

cations in A site, as since Bi^{3+} and Pr^{3+} have the same valence states, therefore the effect of the charge compensation mechanisms is assumed to be negligible, if it already exists. The superposition of all the diffractograms, as shown in Fig.1, reveals, also, a shift to higher 2θ angles in the hkl peak positions, as the rate of Praseodymium substitution increase. Such evolution could be understood considering the variation of the average radii of cations in A site indicated as follows:

$$< r(A) > = (1 - x)\, r(Bi^{3+}) + x\, r(Pr^{3+}) \quad \textbf{(1)}$$

In the coordination XII occupying the A site, the ionic radius of Pr^{3+}, $r(Pr^{3+})$ = 1.13 Å **[30]** is inferior to that of Bismuth, Bi^{3+}, $r(Bi^{3+})$ = 1.17 Å **[30]**.

In fact, theatrical calculation shows a decrease of $< r(A) >$ from 1, 17 Å to 1, 168 Å for $BiFeO_3$ (x = 0) and $Bi_{0.95}Pr_{0,05}FeO_3$ (x = 0,05), respectively, while $< r(B) >$ is kept constant. So, the decrease of the $< r(A) >$, resulting from Praseodymium substitution in A site, induced a 2θ deviation higher angles, resulting in progressive local structural distortion of the unit cell and predicting a decrease in the lattice parameters, therefore of the unit cell volume. To deeper understand these structural distortions and identify the coexistence phases as well structural parameters, the Fullprof program was used to apply Rietveld refinement of X-ray diffraction patterns obtained at room temperature **[40]**. Actually, a progressive isostructural distortion, at room temperature, while maintaining the undoped $BiFeO_3$ parent compound confirmed Rhombohedral structure with R3c space group, for both doped $Bi_{0.975}Pr_{0,025}FeO_3$ (x = 0,025) and $Bi_{0.95}Pr_{0,05}FeO_3$ (x = 0,05) ceramics, with reasonable refinement agreement factors (Table 1). This confirms the progressively increased structural distortion along with the Praseodymium substitution. In fact, the Praseodymium substitution effect on $BiFeO_3$ structural has been widely investigated **[43-47]**: while, S. Pattanayak et al. **[43-44]** and D. Varshney et al. **[45]** confirmed an R3C single phase for the polycrystalline samples of $Bi_{1-x}Pr_xFeO_3$ for $0 \leq x \leq 0.1$ and $0 \leq x \leq 0.15$, respectively. N. Kumar et al. **[45]** reported, for the same $0 \leq x \leq 0.15$ ceramic composition compounds the presence of both R3C and triclinic structures. O. Singh et al. **[49]** proved the mixed symmetry formation for all samples and the transition of crystal structure, as the orthorhombic Pbam phase dominates with the phase fraction reduction of rhombohedral R3c, depending in the sintering time synthesizing. Hence, while all the previous research works investigating the Praseodymium substitution effect on $BiFeO_3$ structural confirm that very low Pr substitution keeps the R3C Rhombohedral structure of the pristine BFO unchanged, the structural transition limit is still controversial (in the range of $0.1 \leq x \leq 0.15$ compositions). This is the basis of $0 \leq x \leq 0.10$ compositions studies for the polycrystalline samples of $Bi_{1-x}Pr_xFeO_3$. In our case, the refinement, lattice parameters and unit cell volume of ceramic compositions are shown in table 1. A significant decrease of the unit cell volume is

reported as the Praseodymium substitution increases, which corroborates the shift of the reflection peaks to 2θ higher angles and works by S. Pattanayak et al. **[43]**. To highlight the role of structural distortion in affecting magnetic and ferroelectric properties, the significant average bond length and angle are tabulated in table 1. Indeed, spontaneous polarization in BFO pristine compound basically results from the stoichiometrically active $6s^2$ lone pairs on Bi^{3+} ions. Further, BFO consists of a network of corner-sharing oxygen octahedral with Fe^{3+} cations inside and Bi^{3+}cations between the cavities. So, as increasing A ion site substitution rate, it is expected that the three long degenerate and the three short degenerate Fe-O band lengths in the R3c octahedral Rhombohedral phase tend to be equal. Y.Wu et al. **[48]** showed that, while increasing the rate of substitution x of Ho^{3+} substituting Bi^{3+} ions, these two band lengths become almost equal (~ 2.03 Å), evidence of the paraelectric Fe displacement, as the symmetry from R3C rhombohedral transits to Pnma orthorhombic. Therefore, based in biography **[43-47]**, Systematic substitution to substitute the Bi^{3+} with smaller amounts of dopants, in our case Pr^{3+}, may distort the cations spacing between octahedral and lead to oxygen octahedral rotation. It can also alter the ferroelectric order in the long run. For that reason, the evolution of Fe-O-Fe band angle, linked to oxygen octahedral rotation and Fe-O average bond length related to the long-range ferroelectric order is extracted, as specified in Table 1, allowing the quantitative follow-up of the ferroelectric evolution. As shown in Table 1, Fe-O-Fe Band angle present a continual increase from 153.30° for BFO pristine sample to 164.71° for x = 0,05 composition compound and Fe-O average bond lengths tend to be almost equal for $Bi_{0.95}Pr_{0,05}FeO_3$ (Fe-O average bond lengths of 2.252(2) Å and 2.120(6) Å for BFO parent compound become of 2.089(2) Å and 2.032(9) Å for x = 0,05 composition ceramic, respectively), as increasing the Pr substitution rate. These structural results predict a ferroelectric properties improvement, as an effect of Pr^{3+} replacing Bi^{3+} ions.

The critical Fe-O-Fe band angle values are reported in table 1. In fact, in a previous work, A. Amouri et al. **[17-19]** proved, with ABO_3 perovskite substitution in BFO, that the magnetization is enhanced thanks to the modulation or the suppression of the cycloid spin structure, depending on the rate of substitution, leading to release the canted magnetic moment due to the increased of the antiferromagnetically canted Fe-O-Fe angle of ordered adjacent planes, G. Catalan et al. **[51]** outline that the improvement of magnetization is due to "chemical pressure." rather than the effect of "unwind" the spiral spin structure of BFO: The difference in ionic radii of Ca^{2+} and Bi^{3+} result in unequal chemical pressure in lattice structure leading to the strengthening of Fe-O-Fe angle signature of powerful antiferromagnetic super-exchange interaction. Hence, G. Catalan et al. **[51]** and also, V.Singh et al. **[50]**, while studding Pr substituting BFO, outline that enhanced magnetic properties and an increase of T_N are correlated to the chemical pressure, in other word to the rate of

substitution. Fe-O-Fe band angle increased in parallel with Pr substitution on BFO. Thus, these structural results predict a magnetic properties improvement, as an effect of Pr^{3+}substutiting Bi^{3+} ions.

2. Magnetic properties

Zero field cooled (ZFC) and field cooled (FC) magnetization measurements of $BiFeO_3$; $Bi_{0.975}Pr_{0,025}FeO_3$ (x = 0,025) and $Bi_{0.95}Pr_{0,05}FeO_3$ (x = 0,05) ceramics has been recorded at a magnetic field of 0,05 T in the temperature range 5-400 K, as shown in Fig.3. Fig.3(a) displays the ZFC and FC magnetizations of our pristine BFO. Both curves are almost coextensive and the magnetization values decrease with temperature down to 200 K, showing conventional antiferrromagnetic nature. As the temperature decreases below 25 K, ZFC and FC magnetization show a significant magnetization increases with decreasing temperature indicating a weak ferromagnetic nature in polycrystalline BFO. These results indicate that spin reorientation could be the origin of a spin ordering change at low temperature in our BFO ceramic. Similar results have been observed in $BiFeO_3$ single crystal **[53]**. Around 250 K, a trivial anomaly is detected, indicating spin glass transition due to the domain wall pining effects **[52-54]**. Conversely, for both x = 0,025 and x = 0,05 composition ceramics, the magnetization is considerably raised compared to that of $BiFeO_3$ parent compound. Also, as shown in Fig.3(b) and (c), an obvious splitting and a clear divergence between the ZFC and FC magnetization curves increases with decreasing temperature, indicating the thermo-magnetic irreversibility phenomena **[54]**, for our BFO Praseodymium doped samples. Such results indicate the vanishing of a true long-range order: G-type antiferromagnetic ordering. This difference between the ZFC and FC magnetization below the antiferro-paramagnetic phase transition (T_N), tabulated in table 1, is a signature of cluster glass phase or spin glass phase, promoting short range interactions over long- range ones **[55]**. These predict the modulation of the antiferrromagnetic spiral spin cycloidal of the pristine BFO, inducing an enhanced magnetic behavior: a ferromagnetic characteristic. Also, while comparing the curves behaviors of $Bi_{0.975}Pr_{0,025}FeO_3$ and $Bi_{0.95}Pr_{0,05}FeO_3$ ceramics to that of the pristine $BiFeO_3$, a gradual enlargement of such difference, as the rate of Pr substitution increased, below T_N. Based in previous report by S. Mukherjee et al. **[55]**, such difference is considerably higher in the cluster glass phase than the spin glass phase. Thus, for our samples, as the rate of Praseodymium substitution increased, a short-range ferromagnetic ordering within a cluster is probably favored.

The temperature dependent magnetization of Pr substituted BFO samples allows us to extracts the values of the magnetic phase transition T_N. T_N which is of 300 K for $Bi_{0.975}Pr_{0,025}FeO_3$ ceramics decresese to be of 230 K for our $Bi_{0.95}Pr_{0,05}FeO_3$ composition solid solution samples. So, T_N decreased as increasing Pr substitution rates, especially when compared to BFO pristine ceramics, T_N ~ 643K **[15-18]**: T_N deviated to room temperature due to substitution with Praseodymium in A site. This deviation continued until for $Bi_{0.975}Pr_{0,025}FeO_3$ ceramics, T_N coincide with room temperature: Such results suggest that Pr substitution can be useful to bring closer the ferroelectric T_c and the magnetic T_N temperatures and improve magnetoelectric coupling **[51, 56-57]**. T_N was expected to increase at higher substitution rates, as Rietveld refinement analysis showed a rise in the Fe-O-Fe band angles. However, it decreased. This evolution of T_N is as follows:

$$T_N = JZS(S+1)\cos\theta$$

with J denotes the magnetic exchange constant, S represents the spin of Fe^{3+}, Z stands for the average number of linkages per Fe^{3+} ions and θ refers to the Fe-O-Fe bond angle.

The T_N decrease is attributed to the low magnetic interactions rather than bond angle variation. A similar result was found by T. Durga Rao et al. **[58]** with Nd and Sc co-substituted $BiFeO_3$.

Fig.4 shows the magnetization versus magnetic field of $BiFeO_3$ parent compound and $(Bi_{1-x}Pr_x)FeO_3$ ceramic system with composition x = 0,025 and x = 0,05. For the pristine BFO, magnetic hysteresis loops, recorded at room temperature, show a nearly linear behavior with small values of remnant magnetization Mr of 0.016 emu/g and a coercive field H_C of about 10 T, signature of a typical AFM antiferrromagnetic behavior, as expected and as reported in literature **[50-51]**. The M-H deviation from linear behaviors, below the freezing temperature, revealing weak ferromagnetism has been attributed by M. K. Singh et al. **[56]**, to spin freezinstudying studding BFO single crystal. These results confirm the effect of the AFM network embedded in spin glass like matrix $BiFeO_3$. Magnetic hysteresis loops, recorded at Room temperature has been superposed, as shown in Fig.4, to deeper investigate the effect of Praseodymium substitution into BFO magnetic properties. The deviation of the linear dependence of magnetization versus magnetic field, for the Pr doped samples is a signature of ferromagnetic behavior, as previously expected through the divergence between the ZFC and FC magnetization curves. Yet the unsaturated hysteresis magnetic loops is attributed to antiferrromagnetic basic nature, the magnetization increased as increasing Pr substituting content in BFO samples prove the co-effect the ferromagnetic ordering spin contribution, resulting in modulating the antiferrromagnetic AFM canted spin, and the AFM ones, embedded in the spin glass like matrix $BiFeO_3$. In fact, for $Bi_{0.975}Pr_{0,025}FeO_3$ ceramic, the magnetic hysteresis loops, showing

signature of both of the persistence of antiferrromagnetic magnetization and the emergence of ferromagnetic order, reveals a remnant magnetization values M_r of 6.73 emu/g. Compared to M_r of 0.016 emu/g, for the pristine BFO, an intensification is reported, as a result of Pr substitution. The improvement of remnant magnetization can be attributed to the substitution which can modulate/suppress the spin cycloidal structure resulting in uncompensated net moment **[59]**. The low values of the magnetization versus magnetic field for $Bi_{0.95}Pr_{0,05}FeO_3$ (x = 0.05) composition ceramic, at room temperature, could be explain as a paramagnetic order (T_N about 230 K, as extracted from ZFC magnetization curves), and not as a decrease resulting from Pr substituting effect. Hence, the increase in magnetization because of Pr substitution could be attributed to the modulation or the suppression, toward a collinear antiferrromagnetic structure **[48]**, of the spiral spin cycloidal structure of pure BFO **[49-50]**. This finding proves the enhancement of the magnetic properties of $BiFeO_3$ at room temperature due to Pr substitution.

3. Ferroelectric properties

Based on previous research **[60-63]**, pure BFO ceramics exhibit weak ferroelectric properties due to its leakage current problem. Although, M. Mahesh Kumar et al. **[60]** reported an attempt to measure ferroelectric hysteresis loop at room temperature, such measurement still challenging and hardly dependent in synthesized parameters **[63]** and measurements **[60-63]**. Such results show a hysteresis loop with an unsaturated remnant polarization of 0.01 $\mu C/cm^2$ and an application of higher fields was restricted due to conductivity of the sample **[60]**. The electric investigation of $Bi_{1-x}Pr_xFeO_3$ polycrystalline solid solutions consisted of a study of dependence of polarization on the electric field (P-E) hysteresis loops at room temperature. Fig.5 (a) and (b) illustrates hysteresis loops of $Bi_{0.975}Pr_{0,025}FeO_3$ (x = 0.025) and $Bi_{0.95}Pr_{0,05}FeO_3$ (x = 0.05), respectively, at the frequency of 10 Hz and a maximum field of ± 50 kV/cm. Although both doped samples showed a different polarization value for the electric field of 0 kV/cm as an aspect of conductivity existent, the polarization grew as a function of applied field according to a nonlinear behavior, characteristic to ferroelectric behavior. So, the enlargement of the area of hysteresis compared to the pristine BFO **[60]** is also proof of the improved ferroelectric property. In fact, as the rate of Pr substitution increased, an enhancement of P-E shape loops is observed. Thus, a deeper looking for $Bi_{0.95}Pr_{0,05}FeO_3$ (x = 0,05) hysteresis loops show a saturation beginning aspect at an applied field of 30 kV/cm. In addition, Pr doping was accompanied by an increase in saturation polarization (P_s) and remnant polarization (P_r): For composition x = 0.05 ceramic, the P_r values, of

12.97 μC/cm^2, demonstrate the improvement of ferroelectric properties, compared to P_r of 0.01μC/cm^2 measured in undoped $BiFeO_3$ ceramic **[60]**, especially with attainable saturation hysteresis loops with P_s of 18.05 μC/cm^2. A.S. Kumar et al. **[64]**, while studding P-E loops of $Bi_{1-x}Pr_xFeO_3$ ($0.0 \leq x \leq 0.2$) samples, showed that the ferroelectric properties are improved with Pr doping in BFO but P-E loops still unsaturated as value of polarization reached a maximum value of 1.02 μC/cm^2 for x = 0.15 composition sample **[64]**. Compared to the values for our $Bi_{0.95}Pr_{0,05}FeO_3$ (x = 0.05) ceramic, our samples show much higher values signature of the improved ferroelectric property. So, it is obvious that Praseodymium substitution leads to electric polarization increased, which proves the improvement of BFO ferroelectric properties with comparatively low leakage current. Thus, these enhanced ferroelectric properties, as the rate of Praseodymium substitution increase, is fully compatible with the tendency to be equal of the three long degenerate and the three short degenerate Fe-O band lengths in our R3c octahedral Rhombohedral phase, previously recorded by XRD measurements, for $Bi_{0.95}Pr_{0,05}FeO_3$ (x = 0.05) ceramics.

4. Magnetoelectric Coupling effect

Extensive efforts are made to optimize the chemical composition and the technical conditions while studying $xBaTiO_3$-(1-x)$BiFeO_3$ system **[47, 65-67]**, in order to maximize their magnetoelectric effect, at room temperature. Such investigation in $Bi_{1-x}Pr_xFeO_3$ solid solutions system has not been evoked, yet. Thus, the magnetoelectric properties of $Bi_{1-x}Pr_xFeO_3$ solid solution was analyzed in term of compositions and poling effects, at room temperature. The results of the linear α_{ME} magnetoelectric coefficient measurements of our prepared ceramics has been recorded at room temperature, with various DC magnetic field, as presented in Fig.6 and Fig.7. In fact, in order to optimize the composition $x_{optimal}$ of our $Bi_{1-x}Pr_xFeO_3$ solid solution ceramics, at room temperature, the variation of the linear magnetoelectric coefficient α_{ME} with H_{DC} of $BiFeO_3$; $Bi_{0.975}Pr_{0,025}FeO_3$ (x = 0.025) and $Bi_{0.95}Pr_{0,05}FeO_3$ (x = 0.05) ceramics was recorded at room temperature and illustrated in Fig.6 (a), (b) and(c), respectively. Normally, BFO, exhibits only a nonlinear effect, seen its spiral spin arrangement **[65]**, nevertheless, a low α_{ME} values that do not exceed 0.1 mV/cmOe has been measured. Such values could be due to the low impurity phases, as detected in XRD, or to defects seen micrometric morphology, as reported by E. Jartych et al. **[67]**. The magnitude of the α_{ME} of a given value of H_{DC} increases for doped Pr samples compared to the parent compound $BiFeO_3$. The value of α_{ME}, which do not exceed 0.1 mV/cmOe , for pure BFO, increase to be of 1,51 mV/cmOe for x = 0.025 composition then decrease to be 0.20 mV/cmOe for x

= 0.05 ones, at an H_{DC} of 0.1 Oe. Thus, the linear magnetoelectric properties of the investigated BFO Praseodymium doped ceramics are strongly dependent on chemical composition. The maximum α_{ME} value, about 31% higher when compared to BFO parent compound, is reported for $Bi_{0.975}Pr_{0,025}FeO_3$ ceramic. So, the optimum composition, presenting the highest magnetoelectric coupling effect, is $x_{optimal}$ = 0.025. Similar attitude of the α_{ME}, revealing an increased flowed by a subsequent decrease as the rate of substitution increased, has been reported by Su-Chul Yang et al. **[66]**, for $BaTiO_3$-$BiFeO_3$ system: The optimum composition BT-0.725BF ceramics, has been reported to exhibit the higher α_{ME} of 0.87 mV/cm.Oe. Such observation has been attributed to local monoclinic distortions within rhombohedral phase. In our case, for our doped samples, micro-local phase evolution could be estimated by the evolution of the band lengths and angles, as revealed by Rietveld refinement, while keeping the macro R3c rhombohedral structure, like the parent compound BFO. At room temperature, the comparison of our obtained linear α_{ME} magnetoelectric values, which is of 1.51 mV/cmOe for H_{DC} equal to 0.1 Oe, for $Bi_{0.975}Pr_{0,025}FeO_3$ (x = 0.025) ceramics, shows highest values than that reported by K. Kowal et al., for $(BiFeO3)_{0.7}$–$(BaTiO3)_{0.3}$ **[47]** and M Mahesh Kumar et al. **[66]**, for BT-0.725BF ceramics, which are of 0.89 mV/cm.Oe for 1000 Oe and 0.87 mV/cm.Oe, respectively. Also, Lu Liu et al. **[68]**, while adapting the strategy of multi-elements co-substitution for $BiFeO_3$ ceramics, reported a magnetoelectric coupling coefficient α_{ME} of 0.96 mV/cmOe in $Bi_{0.86}(La_{0.20}Nd_{0.20}Sm_{0.20}Gd_{0.20}Lu_{0.20})_{0.14}FeO_3$, proving that such new strategy is an approach to improving magnetoelectric coupling. These results reveal obviously that our doped samples presented higher values of the linear α_{ME}, at the same measurements conditions showing that our materials have potential for many innovative applications, such as in steering the magnetic memory by an electric field and vice versa.

Also, for all our samples, the curves of α_{ME} as a function of H_{DC}, do not retracted the same way on reversal magnetic field, revealing a nonlinear behavior but a hysteresis nature: this could be related to the hysteresis behavior of ours BFO doped Pr samples, at room temperature. $Bi_{0.95}Pr_{0,05}FeO_3$ (x = 0.05) ceramics is in the paraelectric phase, at room temperature, usually exhibit a linear behavior, nevertheless, because of magnetic H_{DC} excitation, the curve does not retracted revealing magnetoelectric behavior. similar hysteresis behavior for $(BiFeO_3)_x$–$(BaTiO_3)_{1-x}$ solid solution compositions has been reported by K. Kowal et al. **[47]**.

As the highest ME effect was observed for $Bi_{0.975}Pr_{0,025}FeO_3$ ceramic, the sample was poled in a field of 3 kV/mm at room temperature (~300 K) for 30 mn. After electrical poling of our most promising Pr doped x = 0.025 composition, the measurements of α_{ME} were recorded, at room

temperature, to compare the results before and after poling, as shown in Fig.7. The measurements were carried out twice to obtain recurring results. All recorded α_{ME} as a function of $H_{DC,}$ confirm the hysteresis behavior of our $Bi_{0.975}Pr_{0,025}FeO_3$ ceramic: The second hysteresis loops confirm a hysteresis nature. while comparing the values of the magnetoelectric coefficient α_{ME} before poling and after poling, it is obvious that α_{ME} show higher values after poling the samples: before electrical poling, α_{ME} was of 1.526 $mVcm^{-1}Oe^{-1}$, while, after electrical poling under an electrical field E = 3 kV/mm, the maximum value of α_{ME} becomes of 2.645 $mVcm^{-1}Oe^{-1}$, when E parallel to H_{DC}, and of 2.645 $mVcm^{-1}Oe^{-1}$ when E perpendicular to H_{DC}. These results confirm the linear magnetoelectric coupling in our sample.

IV. conclusions

$Bi_{1-x}Pr_xFeO_3$ polycrystalline solid solution with $0 \leq x \leq 0.05$ compositions were synthesized by a solid-state reaction method under a controlled atmosphere. The structural, magnetic, ferroelectric and magnetoelectric coupling properties have been studied. The Rietveld refinement of XRD data revealed an isostructural rhombohedral R3c structure for all our doped ceramics. The ferroelectric (P versus E) and magnetic (M versus H) hysteresis loop, recorded at room temperature, showed the improvement of both magnetic and ferroelectric properties because of Praseodymium substitution. $Bi_{0.95}Pr_{0,05}FeO_3$ ceramics presents saturated hysteresis loops with a spontaneous polarization (P_s) of 18.05 $\mu C/cm^2$. The deviation of the linear dependence of magnetization versus magnetic field is a signature of ferromagnetic behavior vanishing, while antiferrromagnetic basic nature persists. The ZFC and FC magnetization confirm the rise of short-range interactions over long- range ones predicting the modulation of the antiferrromagnetic spiral spin cycloidal of the pristine BFO. The highest remnant magnetization M_r values was of 6.73 emu/g for $Bi_{0.975}Pr_{0,025}FeO_3$ ceramic compositions. As increasing Pr substitution rates, T_N decreased toward room temperature for $Bi_{0.975}Pr_{0,025}FeO_3$ ceramics suggesting the enhancement of magnetoelectric coupling as ferroelectric temperature T_c and the magnetic T_N become closer. Measurements of the magnetoelectric coupling coefficient α_{ME}, reveals the hysteresis nature. At room temperature, the optimum x = 0.025 ceramic compositions present the highest value of α_{ME}: before electrical poling, α_{ME} was of 1.526 $mVcm^{-1}Oe^{-1}$, while, after electrical poling under an electrical field E = 3 kV/mm, the maximum value of α_{ME} becomes of 2.645 $mVcm^{-1}Oe^{-1,}$ when $E \parallel H_{DC}$, and of 2.645 $mVcm^{-1}Oe^{-1}$ when $E \perp H_{DC}$. Several attractive features, especially linear magnetoelectric coupling,

made our $Bi_{0.975}Pr_{0,025}FeO_3$ magnetoelectric ceramics as a potential candidate in multiple innovative applications.

Acknowledgement

This work was carried out within the framework of the national project *Programme for the Encouragement of Young Researchers* (2024 program), entitled “Optimisation de la Réactivité Électrode-Électrolyte dans les Électrolyseurs Alcalins pour une production efficace d'Hydrogène Vert”. The authors would like to express their sincere gratitude to their socio-economic partner HyO-Tec for their valuable support.

Data Availability Statement

The authors declare that the data supporting the findings of this study are available within the paper.

References

[1] N.A. Hill, Why are there so few magnetic ferroelectrics? J. Phys. Chem. B 104, (2000) 6694-6709.

[2] R. Ramesh, N.A. Spaldin, Multiferroics: progress and prospects in thin films, Nat. Mater. 6 (2007) 21-29.

[3] S.-W. Cheong, M. Mostovoy, Multiferroics: a magnetic twist for ferroelectricity, Nat. Mater. 6 (2007) 13-20.

[4] M. Bibes, A. Barth elemy, Multiferroics: towards a magnetoelectric memory, Nat. Mater. 7 (2008) 425-426.

[5] W. Eerenstein, N.D. Mathur, J.F. Scott, Multiferroic and magnetoelectric materials, Nature 442 (2006) 759-765.

[6] J. T. Heron and T. Chiang, Magnetoelectrics and multiferroics: Materials and opportunities for energy efficient spin-based memory and logic, MRS Bulletin, 10, (2021), 938-945.

[7] J. M. Caicedo, J. A. Zapata, M. E. Gómez, and P. Prieto**,** Magnetoelectric coefficient in $BiFeO_3$ compounds, Journal of Applied Physics 103, (2008), 07E306-1-3.

[8] A. Kumar, K.L. Yadav, S. Kumar, N. Kumar, A. Mishra, N. Kumar, U. Shankar, T. Mehrotra, G. Sharma, R. Kumar, G. D. Adhikary, Magnetic, ferroelectric, and magnetodielectric properties of $BiFeO_3$ ceramic co-doped with Eu and Gd, Journal of Physics and Chemistry of Solids 124, (2019) 19–23.

[9] R. Das, G. G. Khan, and K. Mandal, Enhanced ferroelectric, magnetoelectric, and magnetic properties in Pr and Cr codoped $BiFeO_3$ nanotubes fabricated by template assisted route, Journal of Applied Physics 111, (2012), 104115-1-6.

[10] M. Mostovoy, Multiferroics: different routes to magnetoelectric coupling, nature , npj spintronics review articles, Review Article, 2 :18, (2024) 1-7.

[11] F. Yan, G; Chen, L. Lu, P. Finkel, and J. E. Spanier, Local probing of magnetoelectric coupling and magnetoelastic control of switching in $BiFeO_3$-$CoFe_2O_4$ thin-film nanocomposite, Applied Physics Letters 103, (2013) 042906-1-4.

[12] I. Kallel, H. Khemakhem, Z. Sassi, N. Abdelmoula, E.-K. Hlil and N. Randrianantoandro, The origin of the large magnetoelectric coupling in the ceramic $Ba_{0.1}Bi_{0.9}(Ti_{0.9}Zr_{0.1})_{0.1}Fe_{0.9}O_3$, Journal of Physics D: Applied Physics, 55, 6, (2021), 065303-1-14.

[13] T. Ichinose and H. Naganuma, Insight into the mechanism of bidirectional magnetoelectric effects unveil cycloidal/uncompensated hybrid antiferromagnetic multiferroics, Phys. Rev. Materials 7, (2023), 014405-1-7.

[14] J. Dho, X. Qi, H. Kim, J. L. MacManus-Driscoll, and M. G. Blamir, Large Electric Polarization and Exchange Bias in Multiferroic $BiFeO_3$, Adv. Mater., 18, (2006), 1445–1448.

[15] D. Bensaid, N.-E. Benkhettou, A. Kourdassi, Structural and Electronic Properties of $Bixo_3$ (X = Mn, Fe, Cr), Journal of Modern Physics, 2, 7, (2011), 642-650.

[16] J. R. Teague, R. Gerson, and W. J. James, Dielectric hysteresis in single crystal $BiFeO_3$, Solid State Communications, 8, 13, (1970), 1073-1074.

[17] A. Amouri, M. A. Wederni, N. Abdelmoula, H. Khemakhem, Enhanced multiferroïc properties in $Bi_{(1-x)}Y_{2x/3}[Ti_{0.95}(Yb_{0.5}Nb_{0.5})_{0,05}]_xFe_{(1-x)}O_3$ ceramics, Journal of Alloys and Compounds, 794, (2019), 443-454.

[18] A. Amouri, N. Abdelmoula, H.Khemakhem, Improved multiferroic properties in $(1-x)BiFeO_3$-$xBaTi_{0.95}(Yb_{0.5}Nb_{0.5})_{0,05}O_3$ system ($0 \leq x \leq 0.3$), Journal of Magnetism and Magnetic Materials, 417, (2016) 302–312.

[19] A. Amouri, S. Aydi, N. Abdelmoula, H. Dammak, H. Khemakhem, Evidence of magnetoelectric coupling in $0.9BiFeO_3$-$0.1Ba\ [Ti_{0.95}(Yb_{0.5}Nb_{0.5})_{0,05}]O_3$ ceramic, Journal of Alloys and Compounds 739, (2018), 1065-1079.

[20] C. Wang, M. Takahashi, H. Fujino, X. Zhao, E. Kume, T. Horiuchi, and S. Sakai, Leakage current of multiferroic $(Bi_{0.6}Tb_{0.3}La_{0.1})FeO_3$ thin films grown at various oxygen pressures by pulsed laser deposition and annealing effect, Journal of Applied Physics 99, (2006), 054104-1-5.

[21] D.P. Dutta, O. D. Jayakumar, A. K. Tyagi, K. G. Girija, C. G. S. Pillai and G. Sharma, Effect of doping on the morphology and multiferroic properties of $BiFeO_3$ nanorods, Nanoscale, (2010), 2, 1149–1154.

[22] J. Xu, G. Wang, H. Wang, D. Ding, Y. He, Synthesis and weak ferromagnetism of Dy-doped $BiFeO_3$ powders, Materials Letters 63, (2009), 855–857.

[23] S.-T. Zhang, Y. Zhang, M.-H. Lu, C.-L. Du, Y.-F. Chen, Z.-G. Liu, Y.-Y. Zhu, N.-B. Ming, and X. Q. Pan, Substitution-induced phase transition and enhanced multiferroic properties of $Bi_{1-x}La_xFeO_3$ ceramics, Applied Physics Letters, 88, (2006), 162901-1-3.

[24] Z. Yan, K. F. Wang, J. F. Qu, and Y. Wang, Z. T. Song and S. L. Feng, Processing and Properties of Yb-Doped $BiFeO_3$ Ceramics, Applied Physics Letters, 91, 8, (2007), 082906-1-3.

[25] F. Zeng, G. Fan, M. Hao, Y. Wang, Y. Wen, X. Chen, J. Zhang, W. Lu, Conductive property of $BiFeO_3$–$BaTiO_3$ ferroelectric ceramics with high Curie temperature, Journal of Alloys and Compounds 831, (2020), 154853-1-9.

[26] S.-T. Zhang, Y. Zhang, M. -H. Lu, C.-L. Du, Y.-F. Chen, Z.-G. Liu, Y.-Y. Zhu, N.-Ben Ming, and X. Q. Pan, Substitution-induced phase transition and enhanced multiferroic properties of $Bi_{1-x}La_xFeO_3$ ceramics, Applied Physics Letters 88, (2006), 162901-1-3.

[27] I. Calisir, A. A. Amirov, A. K. Kleppe and D. A. Hall1, Optimisation of functional properties in lead-free $BiFeO_3$-$BaTiO_3$ ceramics through La^{3+} substitution strategy, Journal of Materials Chemistry A 6, 13, (2018), 1-93.

[28] N. Itoh, T. Shimura, W. Sakamoto and T. Yogo, Fabrication and Characterization of $BiFeO_3$-$BaTiO_3$ Ceramics by Solid State Reaction**,** Ferroelectrics, 356, (2007), 19–23.

[29] S. Kumari, D.K. Pradhan, P. T. Das, N. Ortega, K. Pradhan, A. Kumar, J. F. Scott, and R. S. Katiyar, Evidence of strong magneto-dielectric coupling and enhanced electrical insulation at room temperature in Nd and Mn co-doped bismuth ferrite, Journal of Applied Physics 122, (2017), 144102-1-10.

[30] A. Mukherjee, M. Banerjee, S. Basu, M.D. Mukadam, S.M. Yusuf, M. Pal, Enhanced magnetodielectric and multiferroic properties of Er-doped bismuth ferrite nanoparticles, Materials Chemistry and Physics xxx (2015) 1-9.

[31] G. S. Lotey, N. K. Verma, Magnetodielectric properties of rare earth metal-doped $BiFeO_3$ nanoparticles, Journal of Materials Science Materials in Electronics, 24, 10, (2013), 1309-1-9.

[32] S. Kumari, D. K. Pradhan, P. T. Das, N. Ortega, K. Pradhan, A. Kumar, J. F. Scott, and R. S. Katiyar, Evidence of strong magneto-dielectric coupling and enhanced electrical insulation at room temperature in Nd and Mn co-doped bismuth ferrite. Journal of Applied Physics 122, (2017), 144102-1-10.

[33] H. Ao, H. Wu, W. Li, M. Lan, Z. Zeng, Q. Zhang, R. Gao, X. Deng, G. Chen, C. Fu, Z. Wang, X. Lei, W. Cai, Effect of sintering temperatures on the magnetoelectric properties of $Bi_{0.78}La_{0.08}Sm_{0.14}Fe0_{.85}Ti_{0.15}O_3$ ceramics, Processing and Application of Ceramics 16, 2, (2022) 89–96.

[34] A. S. Kumar, P. Kumar, R. Walia, V. Verma, Improved ferroelectric, magnetic and photovoltaic properties of Pr doped multiferroic bismuth ferrites for photovoltaic application, Results in Physics 14 (2019) 102403-1-3.

[**35**] J. Silva, A. Reyes, H. Esparza, H. Camacho and L. Fuentes, $BiFeO_3$: A Review on Synthesis, Doping and Crystal Structure, Integrated Ferroelectrics, 126, (2011), 47–59.

[**36**] W. Eerenstein, N. D. Mathur and J. F. Scott, Multiferroic and Magnetoelectric Materials, Nature 442, (2006), 759–765.

[37] Arti, Sumit Kumar, Parveen Kumar, Rajan Walia, Vivek Verma, Improved ferroelectric, magnetic and photovoltaic properties of Pr doped multiferroic bismuth ferrites for photovoltaic application, Results in Physics 14, (2019), 102403-1-9.

[38] V. Verma, A. Beniwal, A. Ohlan, R. Tripathi, Structural, magnetic and ferroelectric properties of Pr-doped multiferroics bismuth ferrites, Journal of Magnetism and Magnetic Materials, 394, (2015), 385-390.

[39] X. Li, X. Wang, Y. Li, W. Mao, P. Li, T. Yang, J. Yang, Structural, morphological and multiferroic properties of Pr and Co co-substituted $BiFeO_3$ nanoparticles, Materials Letters 90 (2013) 152–155.

[40] S. Pattanayak, R.N.P. Choudhary, And P.R. Das, Effect of Praseodymium on Electrical Properties of $BiFeO_3$ Multiferroic, Journal of Electronic Materials, 43, 2, (2014), 470-478.

[41] T. Roisnel, 2005. Laboratoire de Chimie du Solide et Inorganique Moleculaire 4MR6511, CNRS-Université de Rennes I, version 3.70, May 2004, LLB-LCSIM.

[42] R. Dahiya, A. Agarwal, S. Sanghi, A. Hooda, P. Godara, Structural, magnetic and dielectric properties of Sr and V doped $BiFeO_3$ multiferroics, Journal of Magnetism and Magnetic Materials 385, (2015), 175–181.

[43] S. Pattanayak, A. Priyadarshan, R. Subudhi, R. Kumar Nayak, R. Padhee, Tailoring of electrical properties of $BiFeO_3$ by praseodymium, Journal of Advanced Ceramics 2(3), (2013), 235–241.

[44] S. Pattanayak, R.N.P. Choudhary, A. Piyush, R. Das, Effect of Praseodymium on Electrical Properties of $BiFeO_3$ Multiferroic, Journal of Electronic Materials, 43, 2, (2014), 470-478.

[45] D. Varshney, P. Sharma, S. Satapathy, P.K. Gupta, Structural, magnetic and dielectric properties of Pr-modified $BiFeO_3$ multiferroic, Journal of Alloys and Compounds 584, (2014), 232–239.

[46] N. Kumar, N. Panwar, B. Gahtori, N. Singh, H. Kishan, V.P.S. Awana, Structural, dielectric and magnetic properties of Pr substituted $Bi_{1-x}Pr_xFeO_3$ ($0 \leq x \leq 0.15$) multiferroic compounds, Journal of Alloys and Compounds 501, (2010), L29–L32.

[47] K. Kowal, E. Jartych, P. Guzdek, A. Lisi´N Ska-Czekaj, D. Czekaj, Magnetoelectric effect in $(BiFeO_3)_x$–$(BaTiO_3)_{1-x}$ solid solutions, Materials Science-Poland, 33, 1, (2015), 107-112.

[48] Y. Wu, J. Zhang, X. Chen, X. Chen, Phase evolution and magnetic property of $Bi_{1-x}Ho_xFeO_3$ powders, Solid State Communications 151, (2011), 1936–1940.

[49] O. Singh, A. Kumar, K. Kumar, A. Agarwal, S. Sangh, Sintering time dependent structural and magnetic phase transformations in Pr doped $BiFeO_3$ multiferroics, Journal of Magnetism and Magnetic Materials, 519, (2021), 167412-1-18.

[50] V.Singh, S.Sharma, R. K. Dwivedi, M. Kumar, R. K. Kotnala, Multiferroic and optical properties of Pr-substituted bismuth ferrite ceramics, Phys. Status Solidi A 210, 7, (2013), 1442–1447.

[51] G. Catalan, K. Sardar, N. S. Church, J. F. Scott, R. J. Harrison, and S. A. T. Redfern, Effect of chemical substitution on the Néel temperature of multiferroic $Bi_{1-x}Ca_xFeO_3$, PHYSICAL REVIEW B **79**, (2009), 212415-1-4.

[52] B. Ramachandran and M. S. Ramachandra Rao, Low temperature magnetocaloric effect in polycrystalline $BiFeO_3$ ceramics, Applied Physics Letters 95, (2009), 142505-1-3.

[53] Manoj K. Singh, W. Prellier, M. P. Singh, Ram S. Katiyar, and J. F. Scott, Spin-glass transition in single-crystal $BiFeO_3$, Physical Review B **77**, (2008), 144403-1-5.

[54] V.B. Naik, R. Mahendiran, Magnetic and magnetoelectric studies in pure and cation doped $BiFeO_3$, Solid State Communications 149, (2009), 754-758.

[55] S. Mukherjee and R. Ranganathan, Static and dynamic response of cluster glass in $La_{0.5}Sr_{0.5}CoO_3$, Physical Review B 54, 13, (1996), 9267-9274.

[56] A. Agbelele, D. Sando, I. C. Infante, C. Carrétéro, S. Jouen, J.-M. Le Breton, A. Barthélémy, B. Dkhil, M. Bibes, and J. Juraszek, Insight into magnetic, ferroelectric and elastic properties of strained $BiFeO_3$ thin films through Mössbauer spectroscopy, Appl. Phys. Lett. 109, (2016), 042902-1-5.

[57] A. Marzouki, V. Loyau, P. Gemeiner, L. Bessais, B. Dkhil, A. Megriche, Increase of magnetic and magnetoelectric properties in Co/Mn co-doped $BiFeO_3$ multiferroic, Journal of Magnetism and Magnetic Materials, S0304-8853(19), (2019), 32000-1-16.

[58] P. Kumar, N. Shankhwar, A. Srinivasan, M. Kar, Oxygen octahedra distortion induced structural and magnetic phase transitions in $Bi_{1-x}Ca_xFe_{1-x}Mn_xO_3$ ceramics, J. Appl. Phys. 117 (2015), 194103-1-14.

[59] A. Amouri, M.A. Wederni, N. Abdelmoula, H. Khemakhem, Enhanced multiferroïc properties in $Bi_{(1-x)}Y_{2x/3}[Ti_{0.95}(Yb_{0.5}Nb_{0.5})_{0.05}]_xFe_{(1-x)}O_3$ ceramics, Journal of Alloys and Compounds 794, (2019), 443-454.

[60] M. Mahesh Kumar, V. R. Palkar, K. Srinivas, and S. V. Suryanarayana, Ferroelectricity in a pure $BiFeO_3$ ceramic, Applied Physics Letters 76, 19 (2000), 2763- 2766.

[61] A. Joana Preethi and M. Ragam, Effect of doping in multiferroic BFO: A review, Journal of Advanced Dielectrics, 11, 6, (2021) 2130001-1-17.

[62] Y. Zang, D. Xie, Y. Chen, M. Li, X. Han, T. Ren and D. Plant, Comparative Study on Structural and Ferroelectric Properties of Dual-Site Rare-Earth Ions Substituted Multiferroelectric $BiFeO_3$, Integrated Ferroelectrics: An International Journal, 132, (2012), 30–38.

[63] J. H. Choi, T. Yoshimura, N. Fujimura and C. Cheon, Saturated and Pinched Ferroelectric Hysteresis Loops in $BiFeO_3$ Ceramics, Journal of the Korean Physical Society, 74, 3, (2019), 269-273.

[64] A.S. Kumar, P. Kumar, R. Walia, V. Verma, Improved ferroelectric, magnetic and photovoltaic properties of Pr doped multiferroic bismuth ferrites for photovoltaic application, Results in Physics, 14, (2019), 102403 -1-9.

[65] M Mahesh Kumar, A Srinivas, G S Kumar and S V Suryanarayana, Investigation of the magnetoelectric effect in $BiFeO_3$-$BaTiO_3$ solid solutions, J. Phys.: Condens. Matter 11**,** (1999), 8131–8139.

[66] Su-Chul Yang, Ashok Kumar, Valeri Petkov, and Shashank Priya, Room-temperature magnetoelectric coupling in single-phase $BaTiO_3$-$BiFeO_3$ system, Journal of Applied Physics 113, (2013) 144101-1-5.

[67] E. Jartych, T. Pikula, K. Kowal, J. Dzik, P. Guzdek and D. Czekaj, Magnetoelectric Effect in Ceramics Based on Bismuth Ferrite, Nanoscale Research Letters 11, (2016), 234-2-8.

[68] Lu Liu, Xiao Li Zhu, Xiang Ming Chen, Improved ferroelectricity and magnetoelectric coupling effect of multielements co-substituted $BiFeO_3$ ceramics, Journal of the American Ceramic Society, 107, 2, (2024), 933-944.

Figure captions

Fig.1: Superposition of XRD patterns of $BiFeO_3$; $Bi_{0.975}Pr_{0.025}FeO_3$ (x = 0.025) and $Bi_{0.95}Pr_{0.05}FeO_3$ (x = 0.05) ceramics recorded at room temperature.

Fig.2: Rietveld refinements of XRD patterns of **(a)** $BiFeO_3$; **(b)** $Bi_{0.975}Pr_{0.025}FeO_3$ (x = 0.025) and **(c)** $Bi_{0.95}Pr_{0.05}FeO_3$ (x = 0.05) ceramics recorded at room temperature.

Fig.3: Zero Field Cooled (ZFC) and Field Cooled (FC) magnetization curves of **(a)** $BiFeO_3$; **(b)** $Bi_{0.975}Pr_{0.025}FeO_3$ (x = 0.025) and **(c)** $Bi_{0.95}Pr_{0.05}FeO_3$ (x = 0.05) ceramics under an applied Field of 0.05T.

Fig.4: Superposition of magnetic hysteresis loops of $BiFeO_3$ parent compound and $(Bi_{1-x}Pr_x)FeO_3$ ceramic system with composition x = 0.025 and x = 0.05 recorded at Room temperature.

Fig.5: Ferroelectric hysteresis loops of **(a)** $Bi_{0.975}Pr_{0.025}FeO_3$ (x = 0.025) and **(b)** $Bi_{0.95}Pr_{0.05}FeO_3$ (x = 0.05) ceramics recorded at Room temperature.

Fig.6: Variation of the linear magnetoelectric coefficient α_{ME} with H_{DC} of **(a)** $BiFeO_3$; **(b)** $Bi_{0.975}Pr_{0.025}FeO_3$ (x = 0.025) and **(c)** $Bi_{0.95}Pr_{0.05}FeO_3$ (x = 0.05) ceramics recorded at room temperature.

Fig.7: Variation of the linear magnetoelectric coefficient α_{ME} with H_{DC} of $Bi_{0.975}Pr_{0.025}FeO_3$ (x = 0.025) ceramic **(a)** before poling; **(b)** after poling in E parallel to H_{DC} and **(c)** after poling in E perpendicular to H_{DC} , recorded at room temperature.

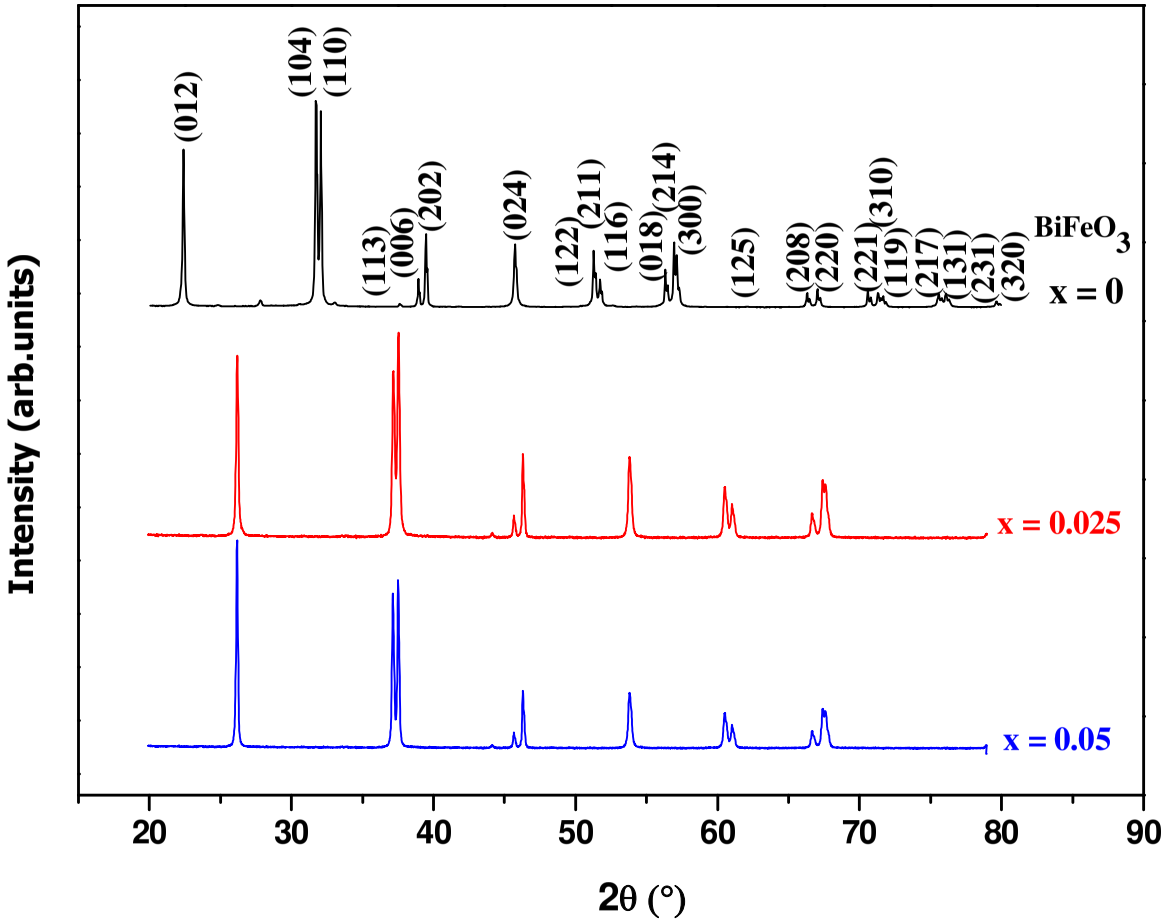

Intensity (arb.units)
(012)
(104)
(110)
(113)
(006)
(202)
(024)
(122)
(211)
(116)
(018)
(214)
(300)
(125)
(208)
(220)
(221)
(310)
(119)
(217)
(131)
(231)
(320)
BiFeO3
x = 0
x = 0.025
x = 0.05
20
30
40
50
60
70
80
90
2θ (°)

Fig.1

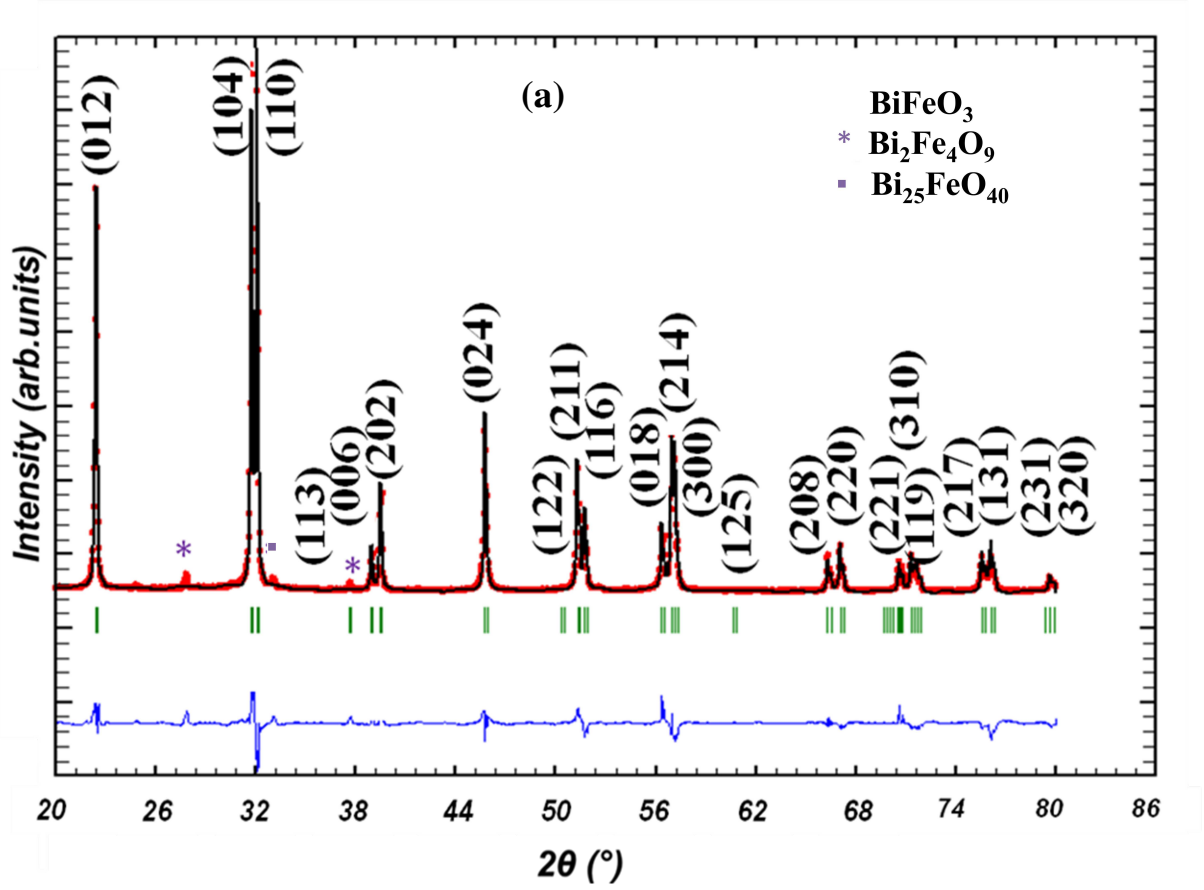

(a)
BiFeO3
* Bi2Fe4O9
▪ Bi25FeO40
(012)
(104)
(110)
(113)
(006)
(202)
(024)
(122)
(211)
(116)
(018)
(214)
(300)
(125)
(208)
(220)
(221)
(119)
(310)
(217)
(131)
(231)
(320)
Intensity (arb.units)
20
26
32
38
44
50
56
62
68
74
80
86
2θ (°)

Fig.2 (a)

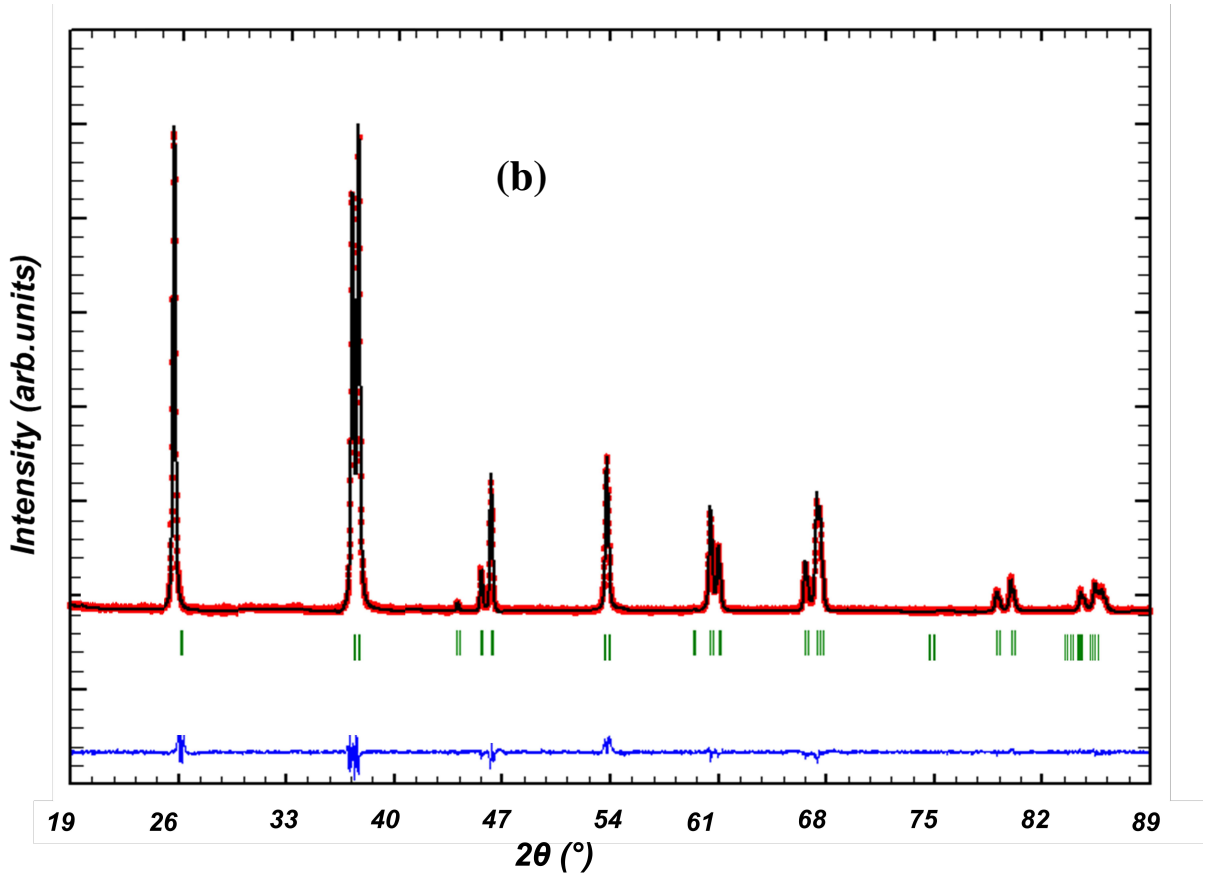


Fig.2 (b)

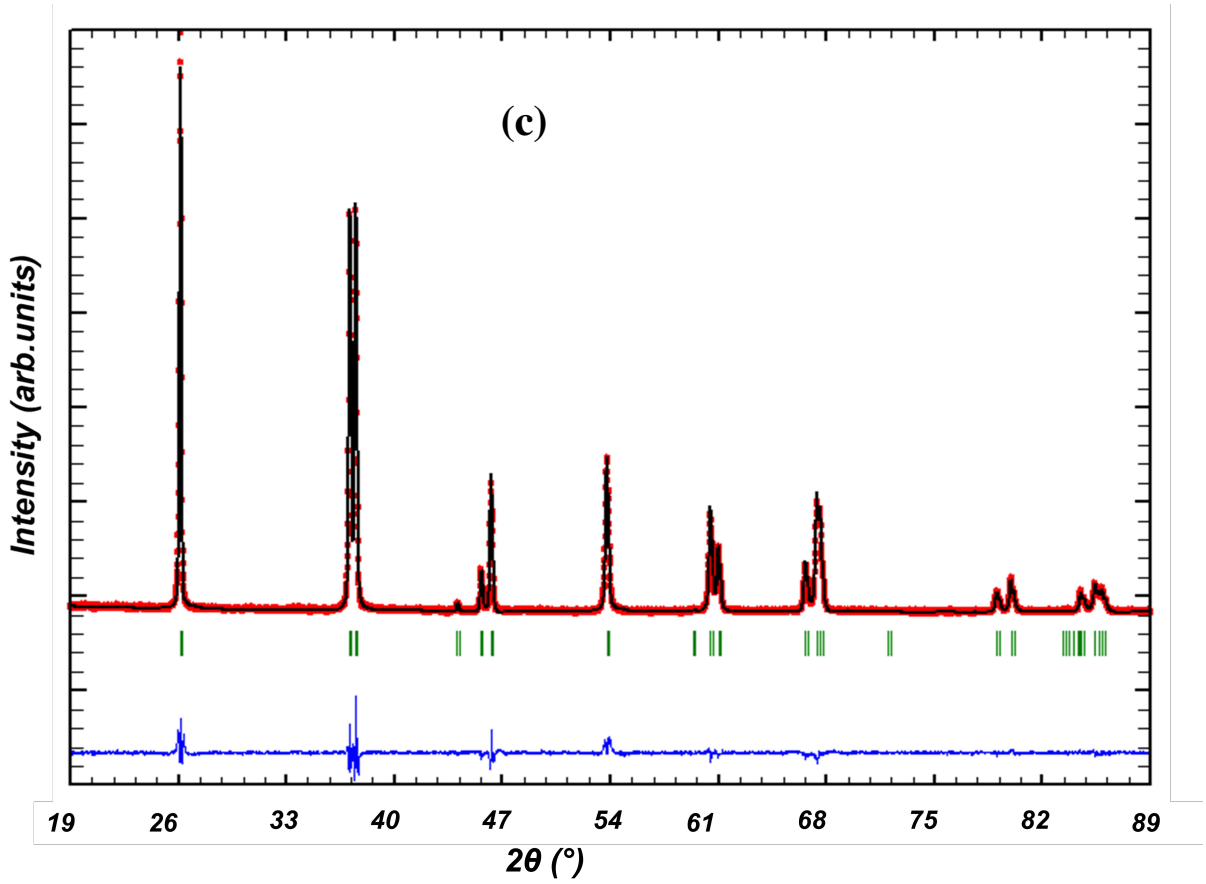


Fig.2 (c)

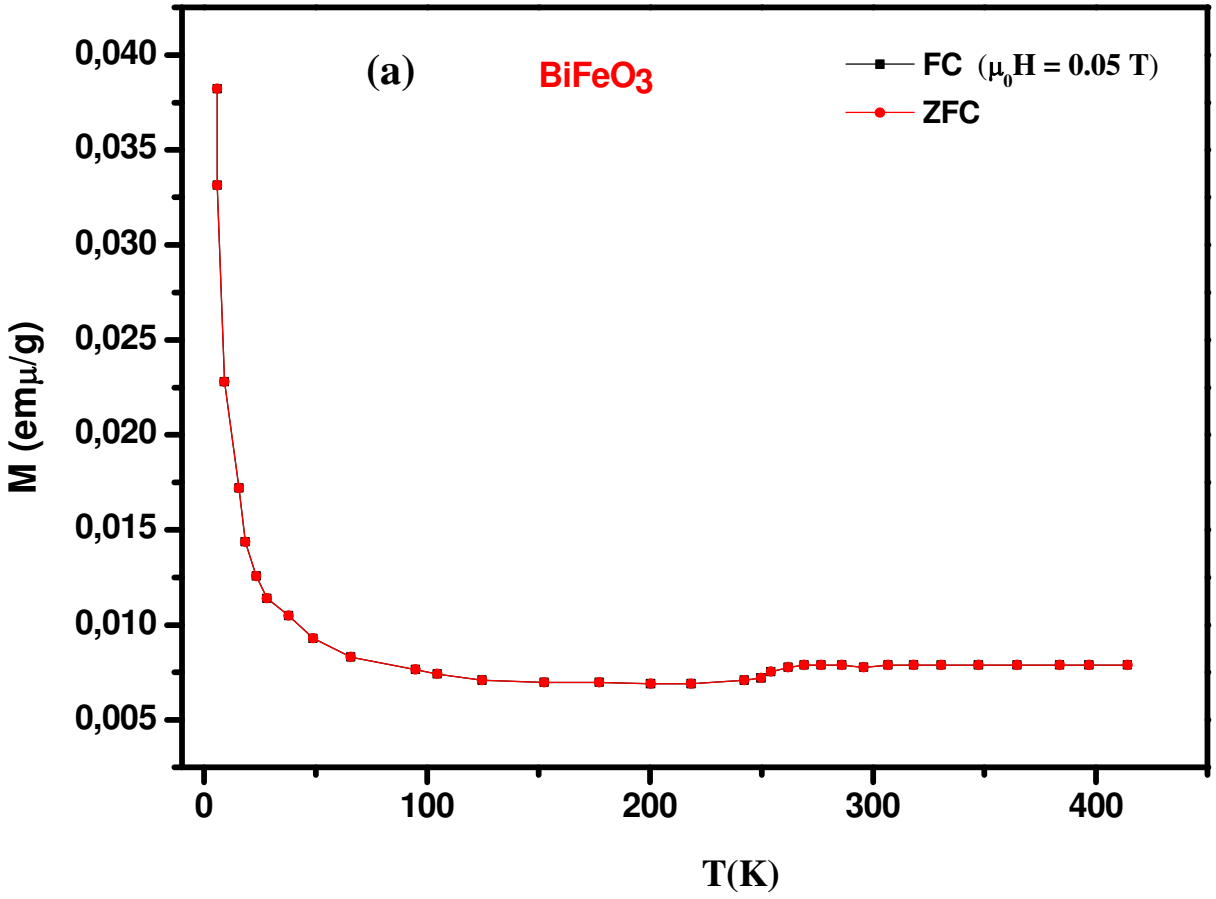

(a)
BiFeO3
FC (μ0H = 0.05 T)
ZFC
M (emμ/g)
0,040
0,035
0,030
0,025
0,020
0,015
0,010
0,005
0
100
200
300
400
T(K)

Fig.3 (a)

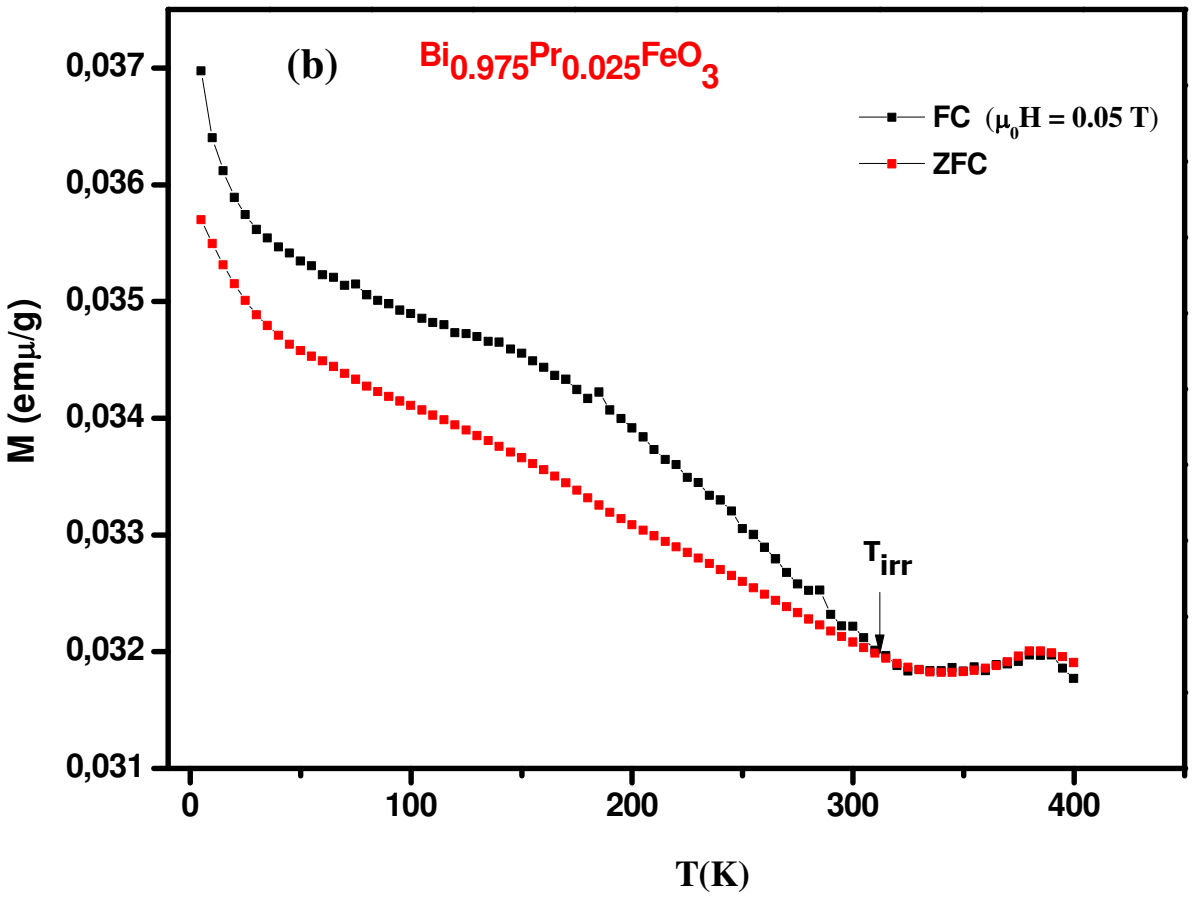

(b)
Bi0.975Pr0.025FeO3
FC (μ0H = 0.05 T)
ZFC
Tirr
M (emμ/g)
T(K)
0,037
0,036
0,035
0,034
0,033
0,032
0,031
0
100
200
300
400

Fig.3 (b)

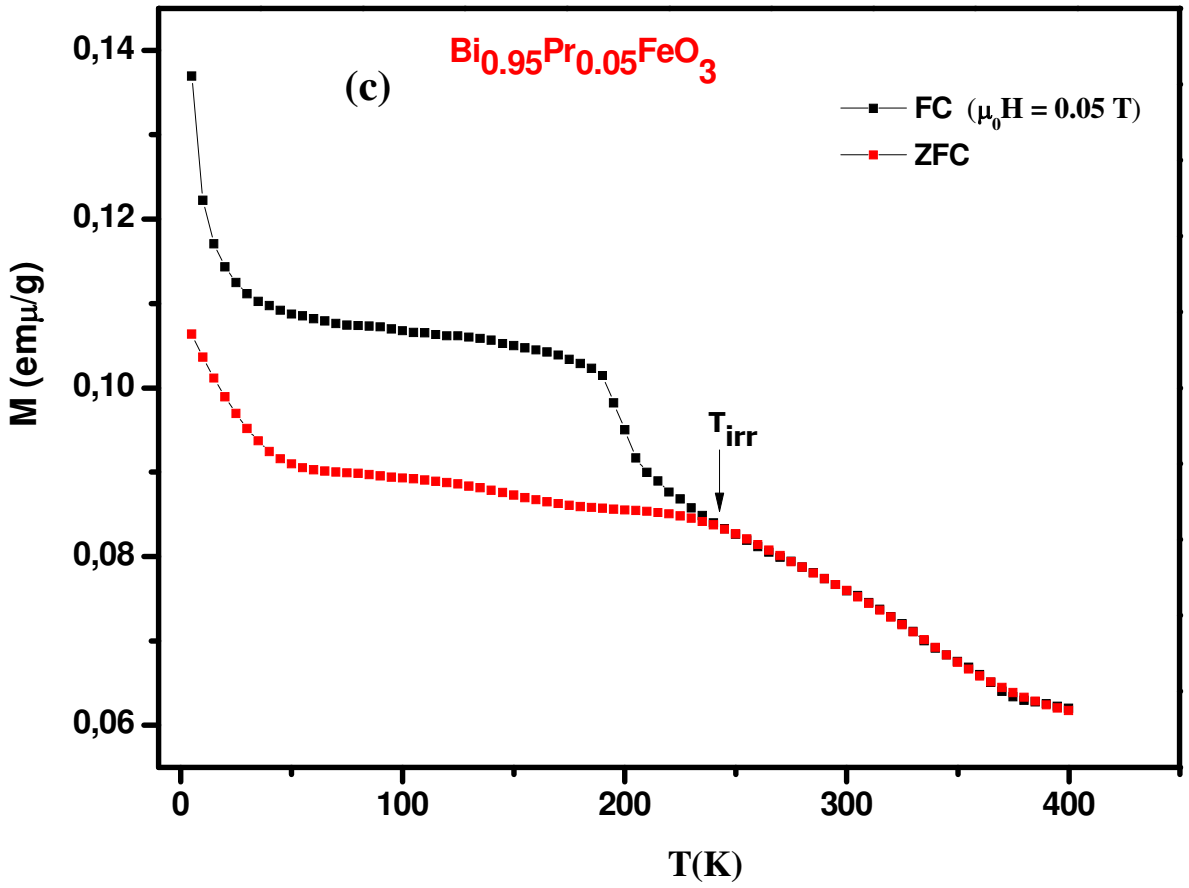

(c)
Bi0.95Pr0.05FeO3
FC (μ0H = 0.05 T)
ZFC
Tirr
M (emμ/g)
T(K)
0,14
0,12
0,10
0,08
0,06
0
100
200
300
400

Fig.3 (c)

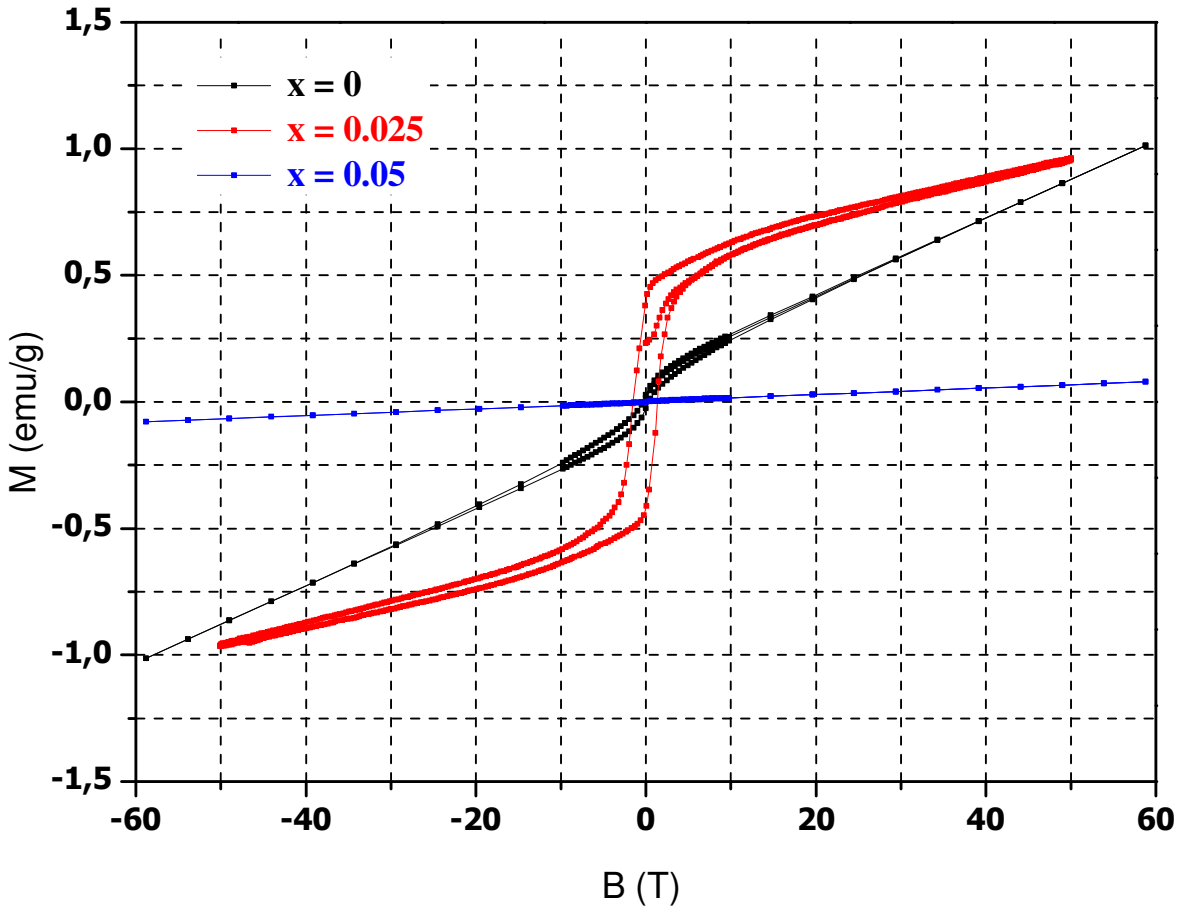


Fig.4

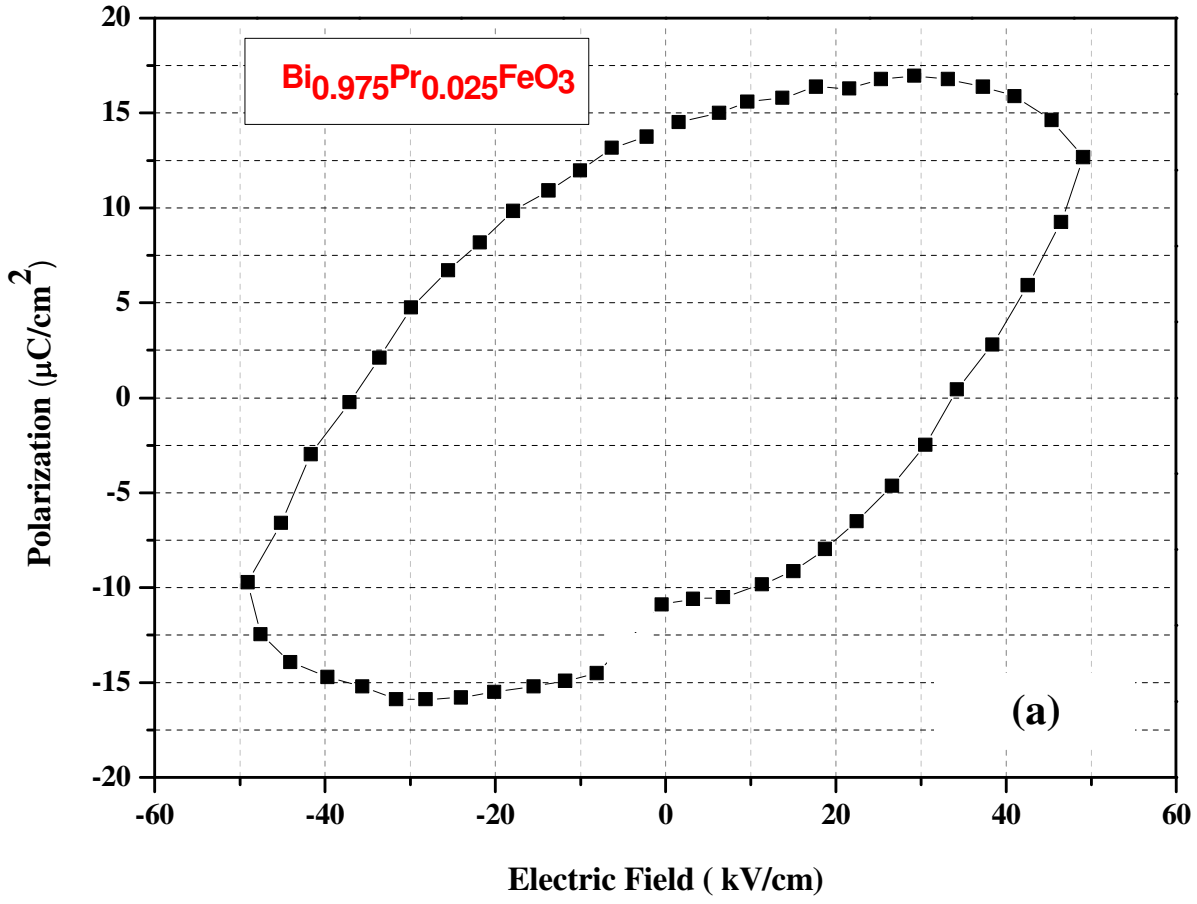

Bi0.975Pr0.025FeO3
Polarization (μC/cm2)
Electric Field (kV/cm)
(a)
20
15
10
5
0
-5
-10
-15
-20
-60
-40
-20
0
20
40
60

Fig.5 (a)

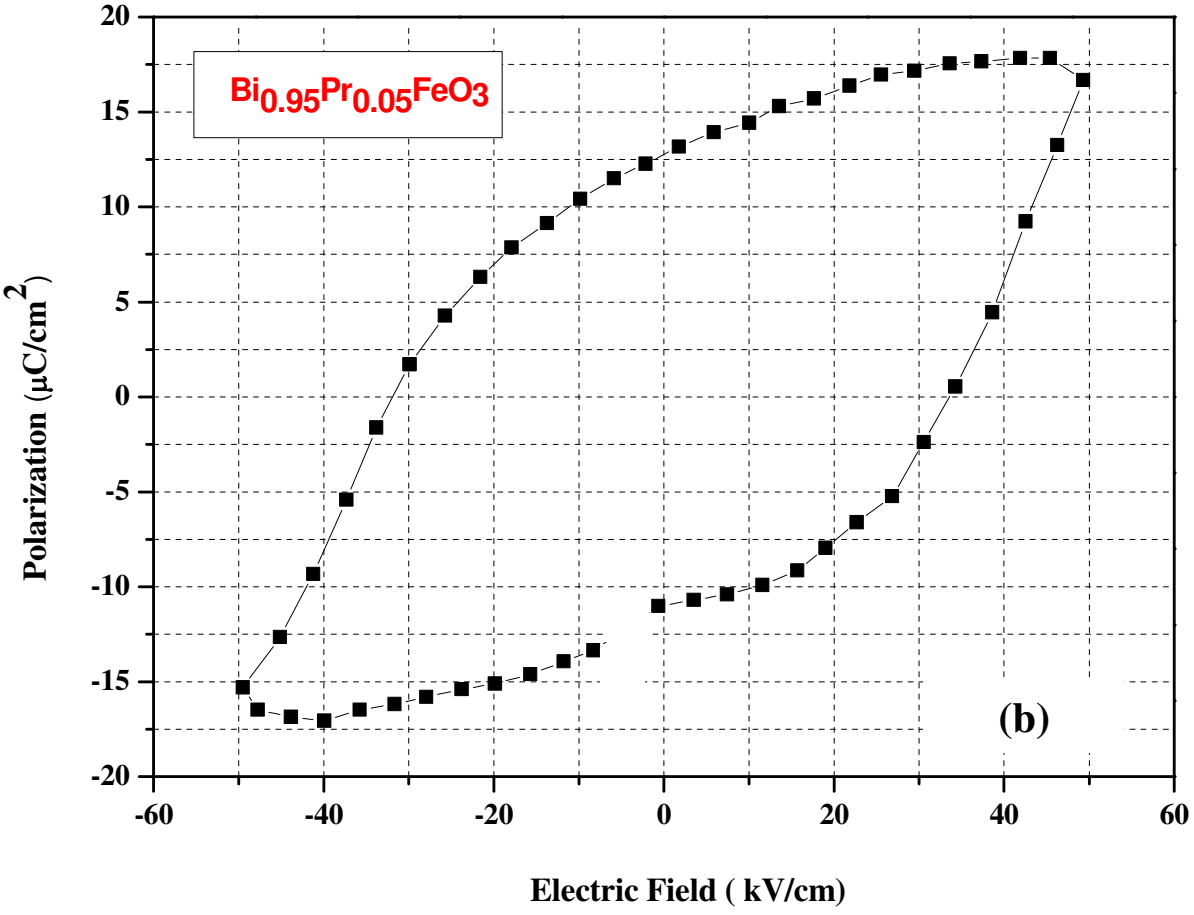

Bi0.95Pr0.05FeO3
(b)
Polarization (μC/cm2)
Electric Field (kV/cm)
20
15
10
5
0
-5
-10
-15
-20
-60
-40
-20
0
20
40
60

Fig.5 (b)

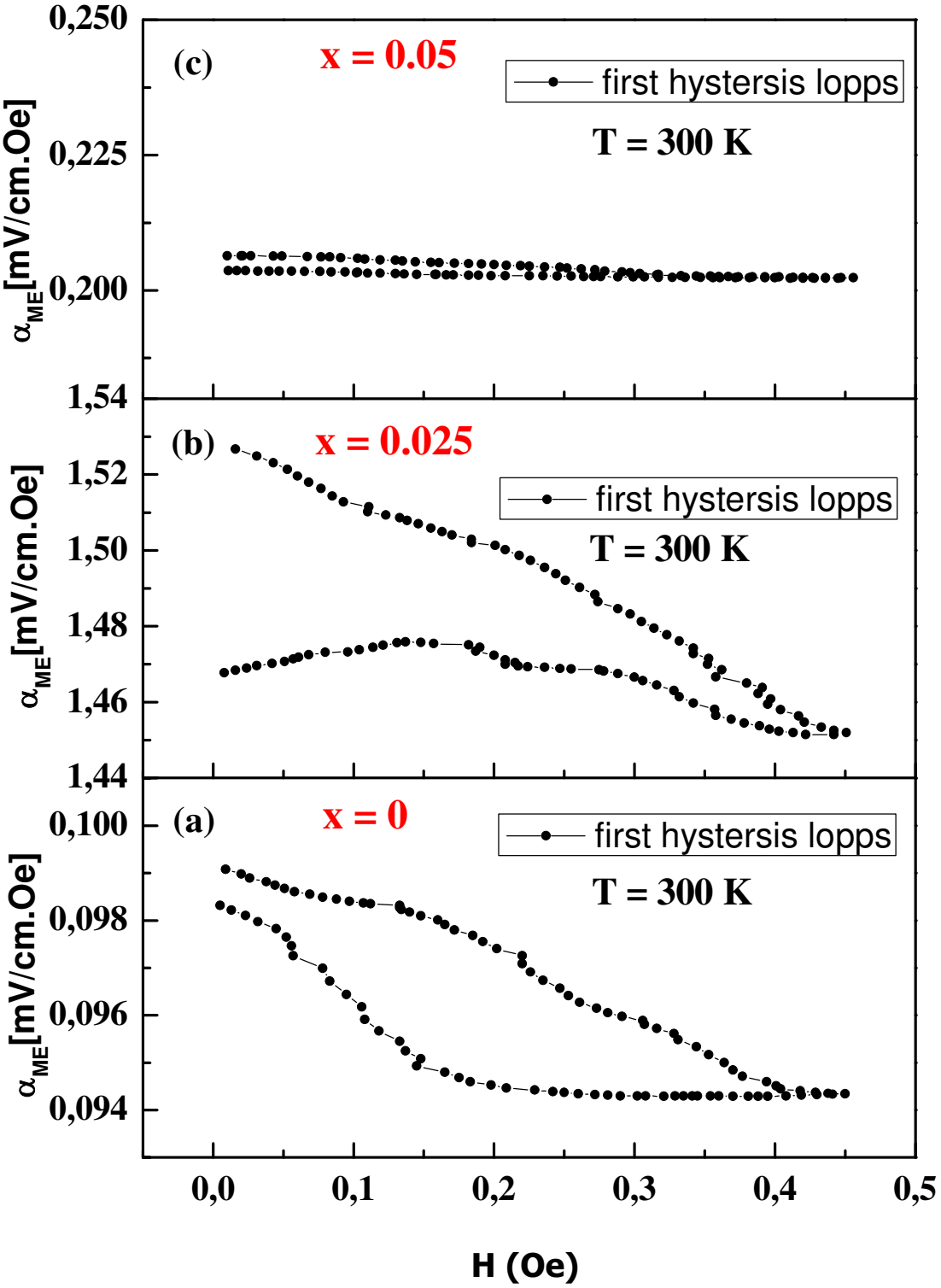

(c)
x = 0.05
first hystersis lopps
T = 300 K
(b)
x = 0.025
first hystersis lopps
T = 300 K
(a)
x = 0
first hystersis lopps
T = 300 K
α_{ME}[mV/cm.Oe]
0,250
0,225
0,200
1,54
1,52
1,50
1,48
1,46
1,44
0,100
0,098
0,096
0,094
0,0
0,1
0,2
0,3
0,4
0,5
H (Oe)

Fig.6

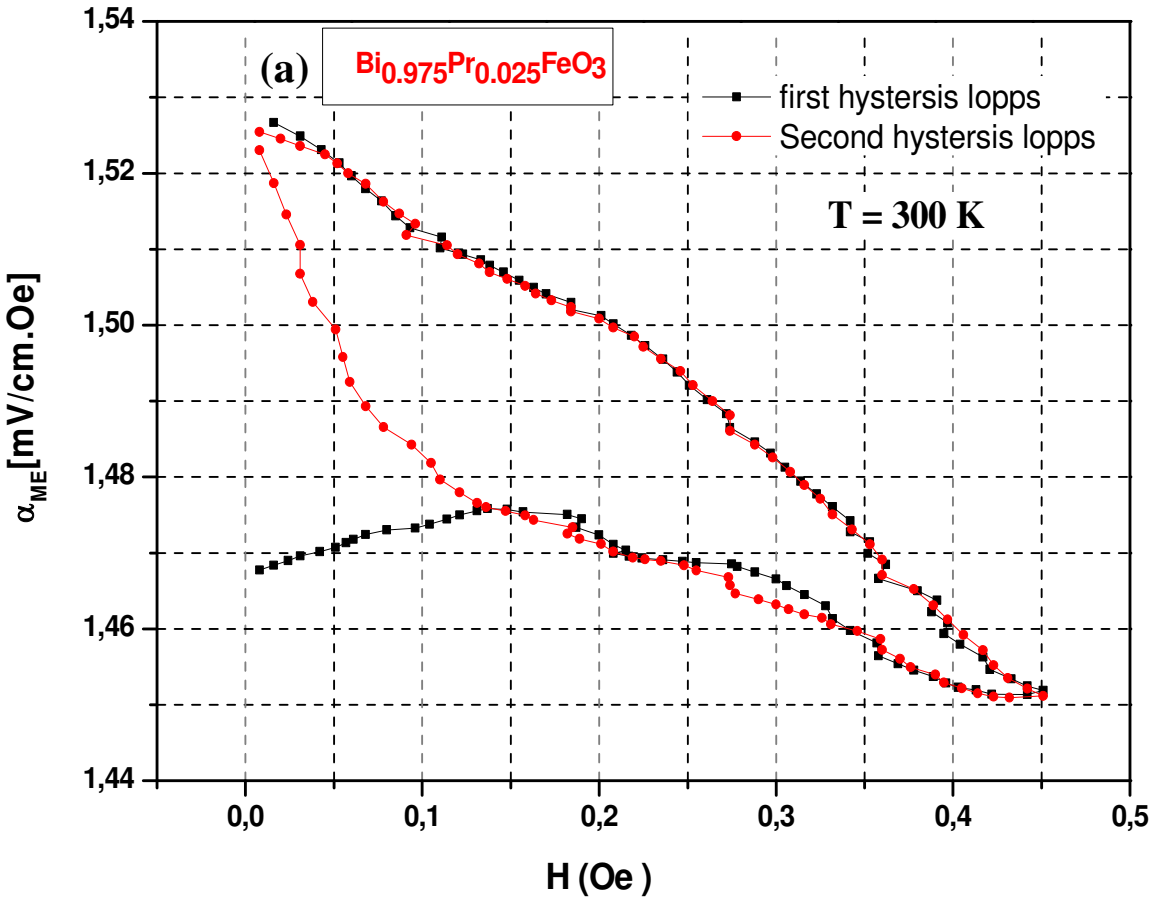

(a)
Bi0.975Pr0.025FeO3
first hystersis lopps
Second hystersis lopps
T = 300 K
αME[mV/cm.Oe]
H (Oe)
1,54
1,52
1,50
1,48
1,46
1,44
0,0
0,1
0,2
0,3
0,4
0,5

Fig.7 (a)

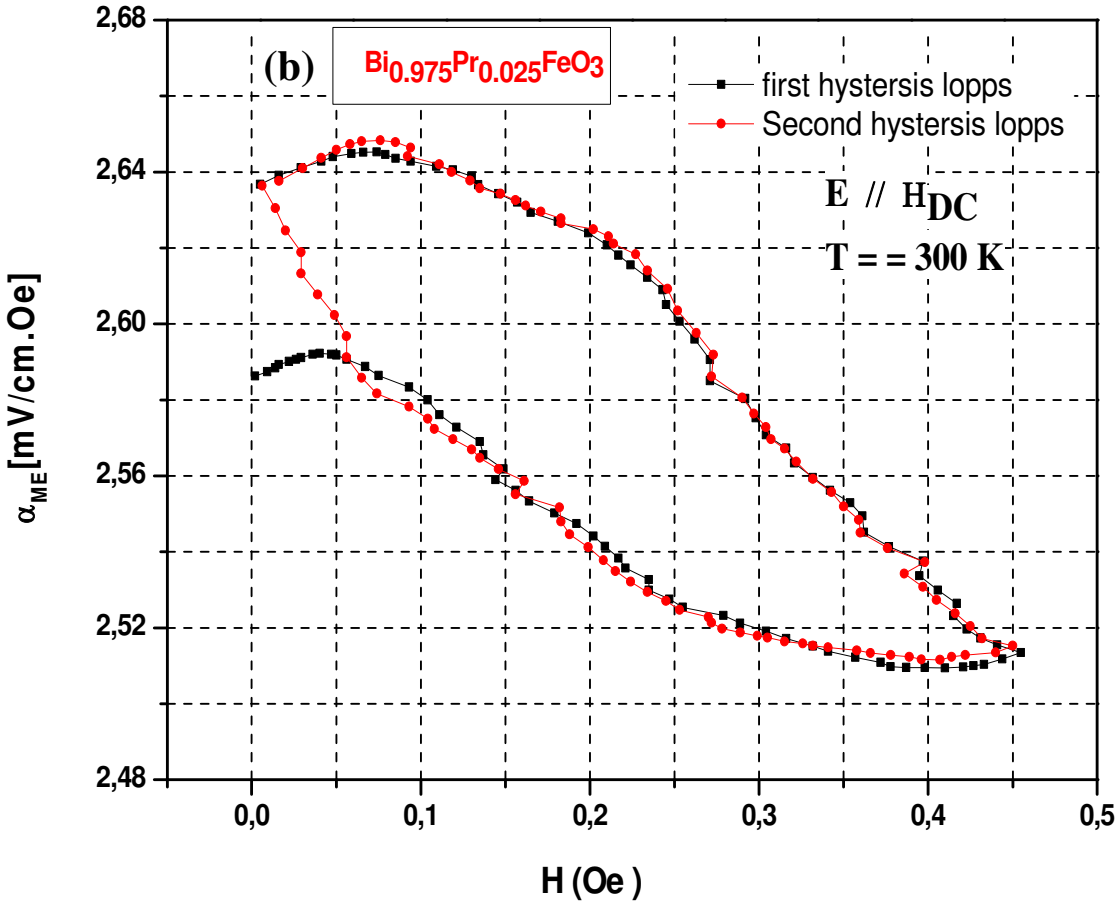

(b)
Bi0.975Pr0.025FeO3
first hystersis lopps
Second hystersis lopps
E // HDC
T = = 300 K
αME[mV/cm.Oe]
H (Oe)
2,68
2,64
2,60
2,56
2,52
2,48
0,0
0,1
0,2
0,3
0,4
0,5

Fig.7 (b)

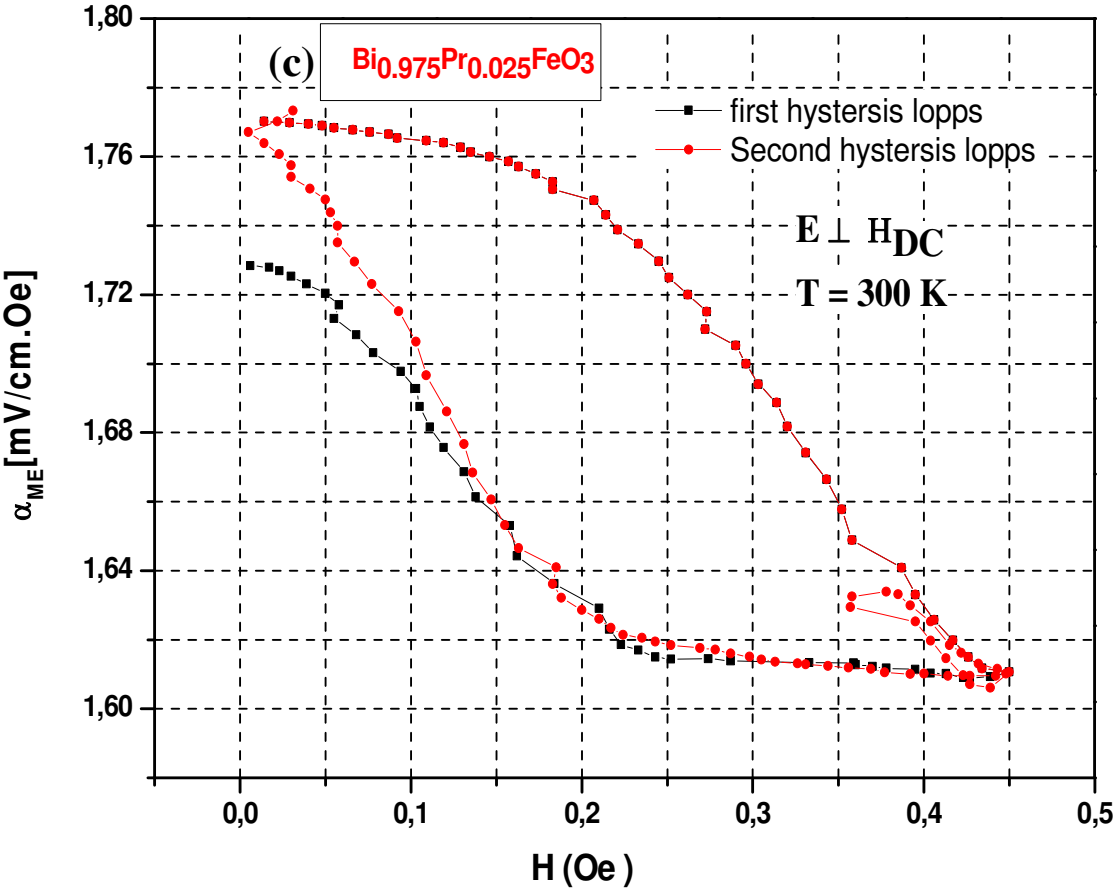

(c)
Bi0.975Pr0.025FeO3
first hystersis lopps
Second hystersis lopps
E ⊥ HDC
T = 300 K
αME[mV/cm.Oe]
H (Oe)
1,80
1,76
1,72
1,68
1,64
1,60
0,0
0,1
0,2
0,3
0,4
0,5

Fig.7 (c)

Table captions

Table 1: Details of Rietveld Refinement structural parameters deduced from XRD and the magnetic transition temperatures extracted from the temperature dependent magnetization, both recorded at room temperature, of $BiFeO_3$ parent compound and $(Bi_{1-x}Pr_x)FeO_3$ ceramic system with composition x = 0.025 and x = 0.05.

Table 1

Compositions (x)	**Crystal Structure**	**Space groupe**	**Cell parameters**	**Average bond length (Å)** **Fe-O**	**Band angle (°)** **Fe-O-Fe**	**R-factor**	$< r(A) >$	**T_N (K)**
0	Rhombohedral	*R3c*	a = b = 5.578(0) Å c = 13.867(6) Å c/a= 2.4861 V = 373.670(6) Å^3	2.252(2) 2.120(6)	153.30	R_p = 8.60 R_{wp} = 11.20 R_{exp} = 4.05 χ = 2.16	1.17	643 K **[11-14]**
0.025			a = b = 5.576(3) Å c = 13.814 (5) Å c/a= 2.4773(5) V = 372.012(9) Å^3	2.153(1) 2.090(3)	156.94	R_p = 6.51 R_{wp} = 8.62 R_{exp} = 4.25 χ = 1.90	1.169	300 K
0.05			a = b = 5.574 (5) Å c = 13.784 (2) Å c/a= 2.472(7) V = 371.957(3) Å^3	2.089(2) 2.032(9)	164.71	R_p = 7.31 R_{wp} = 8.89 R_{exp} = 5.09 χ = 1.82	1.168	230 K